# A pseudopotential hole-particle treatment of neutral rare gas excimer systems. II. The Rydberg states of the $Ar_2^*$ dimer

P. Duplàa and F. Spiegelmann
*Laboratoire de Physique Quantique, UMR 5626 du CNRS, IRSAMC, Université Paul Sabatier, 118 Route de Narbonne, F31462 Toulouse Cedex, France*

(Received 6 February 1996; accepted 10 April 1996)

A pseudopotential hole-particle model (corresponding to the formalism introduced in paper I) is applied to the determination of the Rydberg states of the $Ar_2^*$ excimer with and without spin–orbit coupling. All the $\Lambda$–$\Sigma$ Rydberg states (without spin–orbit coupling) adiabatically dissociating into $Ar+Ar^*$ $(4s,4p,3d,5s,5p,4d)$, are investigated and all $\Omega$ states adiabatically dissociating into $Ar+Ar^*(4s,4p)$ have been determined including spin–orbit coupling. The calculation also includes at short distance attractive molecular configurations diabatically correlated with higher atomic asymptotes. The nature of the $\Lambda$–$\Sigma$ states is analyzed and assigned with reference to the Rydberg orbitals of the $Kr^*$ united atom limit. Extensive comparison with previous calculations and experiments is carried on. For the lowest ungerade states $(1)1_u$, $0_u^-$, $(1)0_u^+$, and $(2)0_u^+$, good quantitative agreement is found with experimental high resolution studies. Several members of Rydberg series are calculated and assigned, yielding intra-Rydberg transition energies $(1)^3\Sigma_u^+((1)1_u,0_u^-)\rightarrow m\,^3\Pi_g$ or $m\,^3\Sigma_g^+$ in good correspondence with recent intra-Rydberg spectroscopy experiments. In particular the present calculation provides a likely interpretation of the infrared spectra of $Ar_2^*$ as due to $(1)^3\Sigma_u^+\rightarrow(1)^3\Sigma_g^+$ transitions with an upper corresponding $\Omega$ state $(1)1_g,0_g^-$ containing quasi-bound vibrational levels. © *1996 American Institute of Physics.* [S0021-9606(96)01927-7]

## I. INTRODUCTION

In the case of dimers, *ab initio* methods have provided a successful approach for most $Rg_2^+$ and $Rg_2^*$ systems which have been investigated by means of configuration interaction (CI) calculations.[1–15] After $Ne_2^{+(1)}$, the $Ar_2^+$, $Kr_2^+$, and $Xe_2^+$ ions were studied by Wadt[2] using frozen-core POL-CI following a self-consistent field (SCF) step. Those ions were also investigated by Michels *et al.*[16] with the local density functional formalism. Spin–orbit (SO) coupling for ions was taken into account in those studies through the atom-in-molecules scheme, first proposed by Cohen and Schneider.[1] Later on, it was shown that the rare gas systems could be approached in the *ab initio* framework by using nonempirical pseudopotentials,[4–14] eventually in the averaged relativistic formulation for the heavier pairs. This reduced the number of active electrons to the valence electrons only and provided a more convenient approach to deal with excited neutral systems. After the frozen-core all electron calculations on $Ne_2^*$ (Ref. 1) and $Ar_2^*$ (Ref. 3), the pseudopotential or effective core pseudopotential techniques were applied to several homonuclear pairs, such as $Ar_2^*$,[6,8,9] $Kr_2^*$,[7,8,14] and $Xe_2^*$.[5]

Further progress in this direction was achieved with the determination and the use of *ab initio* spin–orbit coupling pseudopotentials[11] which allowed for the calculation of fine structure in the $\Omega$ representation by *ab initio* techniques, even in the case of rather heavy systems. This constituted a significant improvement, especially in the case of the electronic structure of neutral excimers, since the straightforward application of the Cohen and Schneider scheme in an adiabatic picture is only valid as long as the adiabatic molecular states retain their asymptotic atomic configurational character. When configuration mixing occurs to become significant, one should apply the Cohen and Schneider method in a diabatic picture or use projection techniques.

Although most of those *ab initio* calculations faces successful comparisons with existing experimental data or even could propose predictions that were later confirmed, one should not hide the difficulties of such calculations. One of the challenges arising in the calculation of the electronic structure of rare gas dimers, even in frozen core or standard pseudopotential scheme, is to achieve a sufficient treatment of the correlation with 15 or 16 electrons. Even on the heavier rare gas atoms, it is sometimes tedious to reach quantitative accuracy for the ionization potentials or the excitation energies from the ground state and the intra- or inter-multiplet splittings can also easily be in error by a few hundred $cm^{-1}$. On the ion pairs, the lack of correlation energy in CI calculations may yield an underestimation of the dissociation energy of the ion ground state, especially when spin–orbit coupling is taken into account. Indeed, the effect of SO coupling is larger at dissociation than in the equilibrium region, where $^2\Sigma_u^+$ and $^2\Pi_u$ states are no longer degenerate. The result is to further reduce the dissociation energy of the $^2\Sigma_{1/2u}$ ground state. The same trend can be observed for the lowest excimer neutral states $1_u$, $0_u^-(^3\Sigma_u^+)$, and $0_u^+(^1\Sigma_u^+)$ which have the same core content as their ground state ionic parents. This trend of course also extends to the whole series of Rydberg states with the same core, when correlation of the valence electrons is not accurately enough accounted for. In neutral excimers, the task is still more difficult, since one has also to account for the interaction of the external electron with the core, thus dealing with very differ-

 0021-9606/96/105(4)/1500/16/$10.00 

ent kinds of situations in the same calculation, with a necessarily large extension of the basis sets (extending from valence to diffuse Rydberg exponents), and the significant work required to achieve consequent CI in such basis sets. Even with the most powerful MRCI codes available today or in recent *ab initio* studies[15] with size-consistent codes specifically dedicated to transition energies, the reach of spectroscopic accuracy for the electronic excited states in a wide energy range is a possible but still difficult challenge and will require further methodological and/or hardware progress.

In paper I,[17] we have developed a hole-particle pseudopotential formalism to deal with rare gas excimer systems. In the present paper (paper II), we examine its numerical application to the $Ar_2^*$ excimer, which can be considered as a test case, since the lowest states were already determined in various *ab initio* studies as previously mentioned and numerous experimental data are available. We however also investigate here higher Rydberg states adiabatically dissociating up to the $3p^5 4d$ configuration in the whole distance range. For the dimer, the model thus couples the degenerate resonant situations, consisting of an electron in an excited molecular orbital in interaction with one $Ar^+$ ion and one neutral Ar atom, that can be obtained through hole transfer. It also allows excitation transfer. The Gaussian $10s/10p/11d$ basis set used in paper I for the check of the $e$-$Ar^+$ pseudopotential was contracted into $6s/5p/4d$ (Table II of paper I). With this basis set, we achieve the determination of all adiabatic $\Lambda$-$\Sigma$ states dissociating into Ar+Ar* ($4s$, $4p$, $3d$, $5s$, $5p$, and $4d$), which also include at short distance, attractive contributions diabatically correlated with higher asymptotes up to Ar+Ar*($6p$). This yields a single hole-particle real matrix ($S_z=0$ only) for the model Hamiltonian with dimension 984. The potential curves in the full distance range ($4a_0<R<10a_0$) are determined with the use of projection techniques (method A of paper I) to approximate the two-electron integrals. However results involving the operatorial technique (method B) are often commented for comparison. When spin–orbit coupling is taken into account, the matrix to be diagonalized is complex and also involves $S_z=1$ and $S_z=-1$ components. Its size is thus doubled. Although all the roots have been obtained, we only discuss here the adiabatic $\Omega$ states adiabatically correlated with Ar+Ar*($4s$,$4p$) (they however include attractive contributions diabatically correlated with higher asymptotes). As mentioned in paper I, spin–orbit coupling concerning the hole is taken into account within a diabaticlike picture, whereas spin–orbit coupling for the excited electron is neglected. The results, the nature of the Rydberg states and the dominant patterns of the electronic structure spectrum are discussed in Sec. II. In particular, correlation of the molecular Rydberg states with the united atom limit is examined. The spectroscopic properties of the lowest states are systematically compared with previous theoretical studies in Sec. III. Finally, Sec. IV achieves an extensive comparison with available experimental data.

## II. NATURE OF THE RYDBERG STATES IN $Ar_2^*$

The potential curves without spin–orbit coupling are displayed in Figs. 1(a)–1(f). Their spectroscopic constants are reported in Table I. The first remark is that singlet and triplet states, at least considered from a diabatic point of view, follow roughly parallel behaviors, as expected, since one deals with Rydberg states. Moreover, the core-Rydberg exchange integrals (associated to the triplet-singlet separation), tend naturally to decrease when the excitation level increases. One can very easily identify at short distance ($R=4.6a_0$) the series of embedded minima corresponding to molecular Rydberg states associated with a $[^2\Sigma_u^+]$ ionic core, the first of which are the lowest excimer states $(1)^{3,1}\Sigma_u^+$ correlated with $Ar^*(4s^{3,1}P)$.

In order to understand qualitatively the general behavior of the potential curves, as well as the nature of the avoided crossings, one can refer back to Mulliken's paper[18] on $Xe_2^*$, and also to the interpretations of the results of actual previous calculations.[1,8] The behavior of the Rydberg states of given space and spin symmetry is determined both by the nature of the core configuration and the evolution of the Rydberg electron molecular orbital (MO). The core parent determines the general form of the potentials ($[^2\Sigma_u^+]$ attractive, $[^2\Pi_g]$ and $[^2\Pi_u]$ moderately repulsive and $[^2\Sigma_g^+]$ very repulsive). One other important feature is the correlation of the Rydberg MOs to the separated atom limit orbitals (SAO) at large internuclear separation and to the orbitals of the united atom (UAO) at short distance. In the case of Ar+Ar*, the united atom limit occurs to be Kr*. As shown by Mulliken, in an adiabatic following, some orbitals are likely to be promoted going from SAO limit to UAO limit, i.e., the number of nodes refering to the UAO limit is increased with respect to the SAO limit. This may imply promotion involving the principal quantum number $n$ and/or the angular moment $l$. However this criterion of the node count should not be too strongly emphasized, because, while the external part of the Rydberg MOs may already have reached a quasiunited atom behavior at the relevant excimer equilibrium distance ($R=4.6a_0$), this is far from being the case for the inner part of the Rydberg orbitals in the atomic core region where the SAO nodal structure remains predominant. Thus, mainly the increase of the node number in the external part of the orbitals is significant. In the present model, based on one-electron pseudopotentials, the lowest SAOs corresponding to different $l$ values (namely $4s$, $4p$, and $3d$) are nodeless and of course only the nodal properties outside the ionic cores are involved. Alternatively to the former adiabatic point of view, one can define qualitative diabaticlike MOs which are basic symmetry combinations of two degenerate SAOs (like in valence bond theory and therefore nonorthogonal). If the parity of the two equivalent SAOs is even ($s,d$...), the gerade combination does not change the nodal structure in the UAO limit, whereas the number of nodes is increased for the ungerade combination. The opposite is true if one considers combinations of odd SAOs ($p,f$...). Since only the unpromoted orbitals can be considered as approximately diabatic, one obtains a very simple qualitative building of diabaticlike

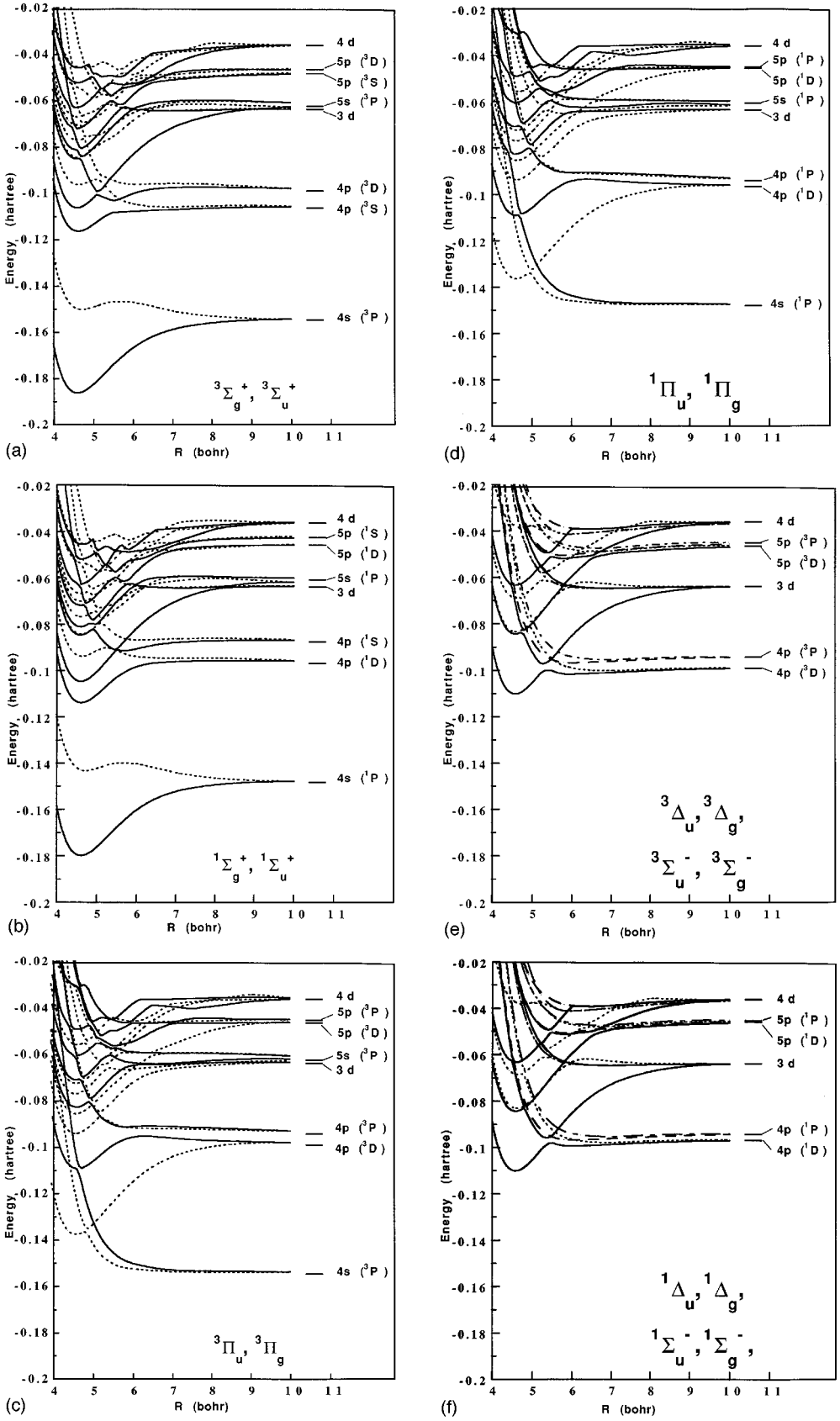


FIG. 1. Potential energy curves of the excited states of $Ar_2^*$ without spin–orbit coupling. (a) $^3\Sigma_u^+$ states (full lines) and $^3\Sigma_g^+$ states (dotted lines); (b) $^1\Sigma_u^+$ states (full lines) and $^1\Sigma_g^+$ states (dotted lines); (c) $^3\Pi_u$ states (full lines) and $^3\Pi_g$ states (dotted lines); (d) $^1\Pi_u$ states (full lines) and $^1\Pi_g$ states (dotted lines); (e) $^3\Delta_u$ states (full lines), $^3\Delta_g$ states (dotted lines), $^3\Sigma_u^-$ states (dashed lines), and $^3\Sigma_g^-$ states (dashed–dotted lines); (f) $^1\Delta_u$ states (full lines), $^1\Delta_g$ states (dotted lines), $^1\Sigma_u^-$ states (dashed lines), and $^1\Sigma_g^-$ states (dashed–dotted lines).

TABLE I. Spectroscopic constants of the $\Lambda-\Sigma$ states of $Ar_2^*$. $R_e$, $\omega_e$, and $\omega_e x_e$ are calculated with method $A$. For the transition energies from $(1)^3\Sigma_u^+(T_e)$ the results of methods $A$ and $B$ are given. The theoretical (CI) values are those of Ref. 8. The experimental (expt.) values are those of Ref. 27 (36 when *).

| State | $R_e$ (Å) | $\omega_e$ ($cm^{-1}$) | $\omega_e x_e$ ($cm^{-1}$) | $T_e$ ($cm^{-1}$) $A$ | $T'_e$ ($cm^{-1}$) $B$ | $T_e$ ($cm^{-1}$) CI | $T_e$ ($cm^{-1}$) Expt. |
|---|---|---|---|---|---|---|---|
| $(1)^3\Sigma_u^+$ | 2.434 | 294 | 2.52 | 0 | 0 | 0 | 0 |
| $(2)^3\Sigma_u^+$ | 2.449 | 283 | 3.48 | 15 326 | 15 089 | 14 312 | |
| $(3)^3\Sigma_u^+$ | 2.434 | 304 | 2.14 | 17 558 | 17 360 | 16 770 | |
| $(4)^3\Sigma_u^+$ | 2.428 | 311 | 2.32 | 22 164 | 21 864 | | |
| $(5)^3\Sigma_u^+$ | 2.429 | 309 | 2.05 | 22 994 | 22 728 | | |
| $(7)^3\Sigma_u^+$ | 2.426 | 312 | 2.36 | 25 013 | 24 792 | | |
| $(8)^3\Sigma_u^+$ | 2.427 | 310 | 2.11 | 27 023 | 26 776 | | |
| $(1)^1\Sigma_u^+$ | 2.433 | 294 | 2.35 | 1349 | 870 | | |
| $(2)^1\Sigma_u^+$ | 2.438 | 294 | 2.84 | 15 819 | 15 530 | 14 971 | |
| $(3)^1\Sigma_u^+$ | 2.434 | 308 | 2.31 | 17 837 | 17 604 | 17 050 | |
| $(4)^1\Sigma_u^+$ | 2.431 | 312 | 1.29 | 22 237 | 22 045 | | |
| $(5)^1\Sigma_u^+$ | 2.429 | 311 | 2.10 | 23 078 | 22 850 | | |
| $(6)^1\Sigma_u^+$ | 2.426 | 313 | 2.11 | 25 021 | 24 824 | | |
| $(8)^1\Sigma_u^+$ | 2.427 | 311 | 2.15 | 27 036 | 26 871 | | |
| $(1)^3\Sigma_g^+$ | 2.496 | 227 | 8.7 | 8010 | 7998 | | 8000* |
| $(2)^3\Sigma_g^+$ | 2.452 | 271 | 9.7 | 19 719 | 19 593 | 18 904 | 19 529 |
| $(3)^3\Sigma_g^+$ | 2.436 | 286 | 3.8 | 22 292 | 22 082 | | 22 003 |
| $(4)^3\Sigma_g^+$ | 2.440 | 291 | 11 | 23 920 | 23 657 | | 23 576 |
| $(5)^3\Sigma_g^+$ | 2.440 | 299 | 7.5 | 25 373 | 25 152 | | |
| $(1)^1\Sigma_g^+$ | 2.497 | 225 | 7.52 | 9465 | 8974 | | |
| $(2)^1\Sigma_g^+$ | 2.448 | 278 | 5.73 | 20 209 | 19 866 | 19 216 | |
| $(3)^1\Sigma_g^+$ | 2.437 | 299 | 2.36 | 22 309 | 22 107 | | |
| $(4)^1\Sigma_g^+$ | 2.436 | 292 | 6.88 | 23 943 | 23 782 | | |
| $(5)^1\Sigma_g^+$ | 2.438 | 304 | 3.28 | 25 387 | 25 193 | | |
| $(1)^3\Pi_u$ | 2.444 | 303 | 2.84 | 16 835 | 16 630 | 15 958 | |
| $(3)^3\Pi_u$ | 2.431 | 302 | 1.08 | 22 674 | 22 476 | 22 002 | |
| $(4)^3\Pi_u$ | 2.428 | 308 | 1.94 | 25 270 | 25 069 | | |
| $(6)^3\Pi_u$ | 2.432 | 300 | 1.93 | 27 547 | 27 363 | | |
| $(1)^1\Pi_u$ | 2.443 | 291 | 2.96 | 16 881 | 16 492 | 16 185 | |
| $(3)^1\Pi_u$ | 2.431 | 305 | 2.10 | 22 683 | 22 501 | 22 101 | |
| $(4)^1\Pi_u$ | 2.429 | 310 | 2.00 | 25 273 | 25 085 | | |
| $(6)^1\Pi_u$ | 2.432 | 296 | 0.92 | 27 558 | 27 373 | | |
| $(1)^3\Pi_g$ | 2.436 | 303 | 2.17 | 10 626 | 10 360 | | 10 110 |
| $(3)^3\Pi_g$ | 2.435 | 305 | 2.74 | 20 160 | 19 945 | 19 305 | 19 830 |
| $(4)^3\Pi_g$ | 2.443 | 296 | 3.02 | 22 058 | 21 853 | | 21 618/ 21 632/ 21 627 |
| $(5)^3\Pi_g$ | 2.434 | 307 | 2.58 | 23 917 | 23 720 | | 23 576 |
| $(1)^1\Pi_g$ | 2.435 | 303 | 2.14 | 10 867 | 10 493 | | |
| $(3)^1\Pi_g$ | 2.437 | 302 | 2.18 | 20 231 | 20 000 | 19 357 | |
| $(4)^1\Pi_g$ | 2.442 | 296 | 2.98 | 22 062 | 21 853 | | |
| $(5)^1\Pi_g$ | 2.435 | 304 | 2.11 | 23 918 | 23 749 | | |
| $(1)^{3,1}\Delta_u$ | 2.421 | 314 | 2.37 | 16 695 | 16 492 | 16 502/16 520 | |
| $(2)^{3,1}\Delta_u$ | 2.423 | 315 | 2.38 | 22 342 | 22 139 | | |
| $(4)^{3,1}\Delta_u$ | 2.422 | 314 | 2.38 | 26 969 | 26 765 | | |
| $(1)^{3,1}\Delta_g$ | 2.429 | 309 | 2.69 | 22 627 | 22 424 | | |
| $(2)^{3,1}\Delta_g$ | 2.434 | 308 | 2.82 | 25 854 | 25 650 | | |

Rydberg states through the association of a given core with an unpromoted diabatic orbital compatible with global spin and space symmetry. Thus the $3p^5ns$ configurations of the separated atoms generate only one unpromoted orbital namely $\sigma_g^*$, and one expects attractive $^{3,1}\Sigma_u^+$ states ($[^2\Sigma_u^+]\sigma_g^*$) configuration), essentially repulsive $^{3,1}\Pi_g$ states ($[^2\Pi_g]\sigma_g^*$ configuration) and $^{3,1}\Pi_u$ states ($[^2\Pi_u]\sigma_g^*$), and very repulsive $^{3,1}\Sigma_g^+$ states ($[^2\Sigma_g^+]\sigma_g^*$). For the $3p^5np$ configurations, the same considerations using the relevant unpromoted diabatic $\sigma_u^*$ and $\pi_u^*$ MOs yield attractive states with $^{3,1}\Sigma_g^+$ and $^{3,1}\Pi_g$ symmetries (configurations $[^2\Sigma_u^+]\sigma_u^*$ and $[^2\Sigma_u^+]\pi_u^*$ respectively), moderately repulsive states with $^{3,1}\Sigma_g^+$, $^{3,1}\Pi_u$, $^{3,1}\Pi_g$, $^{3,1}\Sigma_u^+$, $^{3,1}\Sigma_u^-$, and $^{3,1}\Delta_u$ symmetries (spanned respectively by $[^2\Pi_u]\pi_u^*$, $[^2\Pi_g]\sigma_u^*$, $[^2\Pi_u]\sigma_u^*$, $[^2\Pi_g]\pi_u^*$, $[^2\Pi_g]\pi_u^*$, and $[^2\Pi_g]\pi_u^*$ configurations), and very repulsive states with $^{3,1}\Sigma_u^+$ and $^{3,1}\Pi_u$ symmetries (spanned respectively by $[^2\Sigma_g^+]\sigma_u^*$ and $[^2\Sigma_g^+]\pi_u^*$ configurations). Finally, the $3p^5nd$ configurations generate $\sigma_g^*$, $\pi_g^*$, and $\delta_g^*$ diabatic MOs from which one can built attractive states $^{3,1}\Sigma_u^+$, $^{3,1}\Pi_u$, $^{3,1}\Delta_u$($[^2\Sigma_u^+]\sigma_g^*$, $[^2\Sigma_u^+]\pi_g^*$ and $[^2\Sigma_u^+]\delta_g^*$ respectively), the other ones being essentially repulsive or very repulsive. This provides a kind of diabatic zeroth-order scheme allowing a consistent interpretation of Figs. 1(a)–1(f). Of course, the final potential curves also depend on the character of the avoided crossings between those diabaticlike potential curves. As already discussed by Mulliken[18] and subsequent authors,[1,5–12] the avoided crossings that occurs in the medium and short distance range can be classified within two types. The first one is a case of weakly and very locally avoided crossing, where the two avoiding states are clearly built on configurations which differ through both the core and the particle (two differences). In the bottom of the spectrum and as quoted in previous studies, characteristic examples occur for instance between $(1)^{3,1}\Pi_g$ and $(2)^{3,1}\Pi_g$ and also between $(1)^{3,1}\Pi_u$ and $(2)^{3,1}\Pi_u$ as seen in Figs. 1(c) and 1(d). Other sequential crossings of this type between repulsive states and attractive $[^2\Sigma_u^+]$ core states result in states exhibiting cascades of avoided crossings as obviously seen in all symmetries. The second case concerns strongly avoided crossings for which the lowest $^{3,1}\Sigma_g^+$ states, with a short distance well followed by a barrier, provide a typical illustration. In our above simple interpretation, those states result from a crossing between the diabatic repulsive configuration $[^2\Sigma_g^+]\sigma_g^*4s$ and the attractive $[^2\Sigma_u^+]\sigma_u^*4p$ one. Figure 2 provides the core content of the adiabatic $^{3,1}\Sigma_g^+$ states. At asymptotically large distance, both states have equal occupations on the degenerate configurations $[^2\Sigma_u^+]\sigma_u^*4s$ and $[^2\Sigma_g^+]\sigma_g^*4s$. Consistently with the previous interpretation, the weight on configuration $[^2\Sigma_u^+]\sigma_u^*$ first tends to decrease in the region down to $R=8a_0$ and the states behave repulsively in the long range. However, the upper attractive diabatic state involved in the crossing has $[^2\Sigma_u^+]\sigma_u^*4p$ nature and overlaps very strongly with $[^2\Sigma_u^+]\sigma_u^*4s$, inducing actually a strong coupling resulting into a slow and progressive core transformation as shown in Fig. 2. The upper state of the avoided crossing becomes completely repulsive at short distance, before it undergoes

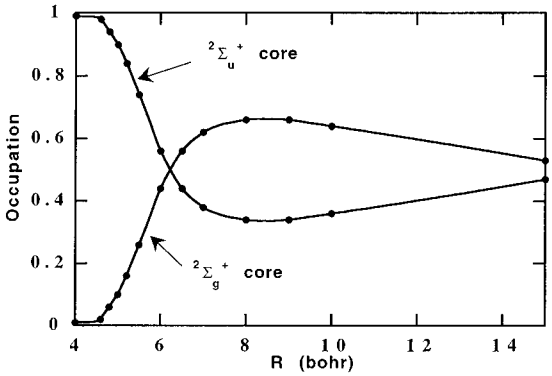


FIG. 2. Evolution of the core nature (occupation number) of the (1) $^{3,1}\Sigma_g^+$ state as a function of interatomic distance.

further avoided crossing with higher attractive configurations. Equivalent adiabatic explanation can be given in terms of adiabatic promotion, since in the adiabatic picture, the MO $\sigma_u^*4s$ transforms slowly into a $p_\sigma$ orbital of the united atom. The humps in (3) $^3\Sigma_u^+$, $(2)^{3,1}\Pi_u$, and $(2)^3\Delta_g$ around $R=7a_0$ are caused by the same processes. It is to be noticed that for the latter states, those humps appear at larger distance than for the lower states. This is due to the fact that the excited orbitals for those states are more diffuse and the interaction switches on at longer distance as the excitation level increases.

In order to quantify this qualitative assignment and also because of the observation of some of those short distance bound states in inter-Rydberg absorption experiments, we have achieved an UAO analysis in the following way. We have computed the one-particle density matrix and the natural orbitals for each adiabatic excited state. Since the core is treated via a minimal hole basis set representation, this provides directly the core nature. As concerns the natural orbital, the assignments of Rydberg states in terms of the UAO limit were analyzed by computing the overlaps of these natural MOs at $R=4.6a_0$ with the atomic orbitals of the Krypton atom (also obtained via $e$-$Kr^+$ one-electron and core-polarization pseudopotentials). The results are presented in Table II.

For most states listed and at this distance, the analysis provides a well-defined nature of the core with a hole orbital occupation number generally in the range of 0.96–0.99. This rule admits a few exceptions as one can see in Table II for some of the higher excited states, due essentially to mixings of $[^2\Pi_u]$ and $[^2\Pi_g]$ cores (associated with Rydberg MO of consistent symmetries).

The lowest $^{3,1}\Sigma_u^+$ excimer states receive a unique assignment in terms of the $5s$ UAO of Kr*. However, in this symmetry, mixtures appear in higher states. Thus (2) $^{3,1}\Sigma_u^+$ and (3) $^{3,1}\Sigma_u^+$ states involve a $[^2\Sigma_u^+]$ core associated with a combination of both $4d_\sigma$ and $6s$ orbitals. The same situation occurs for (4) $^{3,1}\Sigma_u^+$ and (5) $^{3,1}\Sigma_u^+$ states involving mixings of $5d_\sigma$ and $7s$ orbitals or for (6) $^1\Sigma_u^+$ and (7) $^3\Sigma_u^+$ states in which $8s$, $6d_\sigma$, and $7d_\sigma$ orbitals have nonvanishing contributions. Those embedded attractive states are crossed by re-

TABLE II. Nature of the $\Lambda-\Sigma$ states of $Ar_2^*$ at $R=4.6\ a_0$. The most occupied natural MO of the excited particle is analyzed in terms of the united atom orbitals of Kr*. $\Delta_{ST}^A$ and $\Delta_{ST}^B$ are the triplet–singlet separations corresponding to methods $A$ and $B$ respectively for computing the two-electron integrals.

| | Core | Excited particle | Occupation | $\Delta_{ST}^A$ ($cm^{-1}$) | $\Delta_{ST}^B$ ($cm^{-1}$) |
|---|---|---|---|---|---|
| $(1)^{3,1}\Sigma_u^+$ | $[^2\Sigma_u^+]$ | $0.97\ \|5s\rangle$ | 0.98 | 1349 | 870 |
| $(2)^{3,1}\Sigma_u^+$ | $[^2\Sigma_u^+]$ | $0.78\|4d_\sigma\rangle+0.51\|6s\rangle$ | 0.97 | 493 | 440 |
| $(3)^{3,1}\Sigma_u^+$ | $[^2\Sigma_u^+]$ | $0.41\|4d_\sigma\rangle-0.83\|6s\rangle$ | 0.99 | 278 | 243 |
| $(4)^{3,1}\Sigma_u^+$ | $[^2\Sigma_u^+]$ | $0.77\|5d_\sigma\rangle-0.55\|7s\rangle$ | 0.99 | 73 | 180 |
| $(5)^{3,1}\Sigma_u^+$ | $[^2\Sigma_u^+]$ | $0.45\|5d_\sigma\rangle+0.73\|7s\rangle$ | 0.99 | 12 | 121 |
| $(6)^3\Sigma_u^+$ | $[^2\Pi_g]$ | $0.99\|5p_\Pi\rangle$ | 0.96 | | |
| $(6)^1\Sigma_u^+$ | $[^2\Sigma_u^+]$ | $0.21\|8s\rangle+0.79\|6d_\sigma\rangle+0.27\|7d_\sigma\rangle$ | 0.99 | | |
| $(7)^3\Sigma_u^+$ | $[^2\Sigma_u^+]$ | $0.20\|8s\rangle+0.79\|6d_\sigma\rangle+0.27\|7d_\sigma\rangle$ | 0.99 | | |
| $(7)^1\Sigma_u^+$ | $[^2\Pi_g]$ | $0.99\|5p_\Pi\rangle$ | 0.98 | | |
| $(1)^{3,1}\Sigma_g^+$ | $[^2\Sigma_u^+]$ | $0.98\|5p_\sigma\rangle$ | 0.96 | 1454 | 976 |
| $(2)^{3,1}\Sigma_g^+$ | $[^2\Sigma_u^+]$ | $0.99\|6p_\sigma\rangle$ | 0.98 | 490 | 273 |
| $(3)^{3,1}\Sigma_g^+$ | $[^2\Sigma_u^+]$ | $0.96\|4f_\sigma\rangle$ | 0.99 | 17 | |
| $(4)^{3,1}\Sigma_g^+$ | $[^2\Sigma_u^+]$ | $0.98\|7p_\sigma\rangle$ | 0.98 | 23 | 125 |
| $(5)^{3,1}\Sigma_g^+$ | $[^2\Sigma_u^+]$ | $0.17\|4f_\sigma\rangle+0.76\|5f_\sigma\rangle$ | 0.99 | 10 | 41 |
| $(6)^{3,1}\Sigma_g^+$ | $[^2\Sigma_u^+]$ | $0.94\|8p_\sigma\rangle$ | 0.98 | 15 | 44 |
| $(7)^3\Sigma_g^+$ | $[^2\Pi_u]$ | $-0.94\|5p_\Pi\rangle$ | 0.64 | | |
| | $[^2\Pi_g]$ | $0.99\|4d_\Pi\rangle$ | 0.36 | | |
| $(8)^1\Sigma_g^+$ | $[^2\Pi_u]$ | $-0.94\|5p_\Pi\rangle$ | 0.64 | | |
| | $[^2\Pi_g]$ | $0.99\|4d_\Pi\rangle$ | 0.36 | | |
| $(10)^{3,1}\Sigma_g^+$ | $[^2\Pi_u]$ | $0.99\|5p_\Pi\rangle$ | 0.36 | | |
| | $[^2\Pi_g]$ | $-0.94\|4d_\Pi\rangle$ | 0.64 | | |
| $(1)^{3,1}\Pi_u$ | $[^2\Sigma_u^+]$ | $0.90\|4d_\pi\rangle$ | 0.98 | 46 | 63 |
| $(2)^{3,1}\Pi_u$ | $[^2\Pi_u]$ | $0.97\|5s\rangle$ | 0.66 | 1297 | 1198 |
| | $[^2\Pi_g]$ | $0.98\|5p_\sigma\rangle$ | 0.34 | | |
| $(3)^{3,1}\Pi_u$ | $[^2\Sigma_u^+]$ | $0.87\|5d_\pi\rangle$ | 0.99 | 9 | 25 |
| $(4)^{3,1}\Pi_u$ | $[^2\Sigma_u^+]$ | $0.85\|6d_\pi\rangle$ | 0.97 | 3 | 16 |
| $(5)^{3,1}\Pi_u$ | $[^2\Pi_u]$ | $0.87\|5s\rangle-0.47\|4d_\sigma\rangle$ | 0.62 | 296 | 121 |
| | $[^2\Pi_g]$ | $0.93\|5p_\sigma\rangle$ | 0.38 | | |
| $(6)^{3,1}\Pi_u$ | $[^2\Sigma_u^+]$ | $0.61\|7d_\pi\rangle$ | 0.98 | 11 | 16 |
| $(1)^{3,1}\Delta_u$ | $[^2\Sigma_u^+]$ | $0.96\|4d_\delta\rangle$ | 0.98 | | |
| $(2)^{3,1}\Delta_u$ | $[^2\Sigma_u^+]$ | $0.95\|5d_\delta\rangle$ | 0.99 | | |
| $(3)^{3,1}\Delta_u$ | $[^2\Pi_g]$ | $0.99\|5p_\pi\rangle$ | 0.94 | 491 | 389 |
| $(4)^{3,1}\Delta_u$ | $[^2\Sigma_u^+]$ | $0.76\|6d_\delta\rangle$ | 0.97 | | |
| $(5)^{3,1}\Delta_u$ | $[^2\Pi_g]$ | $0.93/6p_\pi\rangle$ | 0.94 | 108 | 31 |
| $(1)^{3,1}\Sigma_u^-$ | $[^2\Pi_g]$ | $0.99\|5p_\pi\rangle$ | 0.94 | | |
| $(1)^{3,1}\Pi_g$ | $[^2\Sigma_u^+]$ | $0.99\|5p_\pi\rangle$ | 0.99 | 241 | 133 |
| $(2)^{3,1}\Pi_g$ | $[^2\Sigma_u^+]$ | $0.97\|5s\rangle$ | 0.98 | 1375 | 1091 |
| $(3)^{3,1}\Pi_g$ | $[^2\Sigma_u^+]$ | $0.97\|6p_\pi\rangle$ | 0.99 | 71 | 56 |
| $(4)^{3,1}\Pi_g$ | $[^2\Sigma_u^+]$ | $0.90\|4f_\pi\rangle$ | 0.98 | 4 | 0.5 |
| $(5)^{3,1}\Pi_g$ | $[^2\Sigma_u^+]$ | $0.92\|7p_\pi\rangle$ | 0.99 | | |
| $(6)^{3,1}\Pi_g$ | $[^2\Sigma_u^+]$ | $0.33\|7p_\pi\rangle+0.62\|5f_\pi\rangle$ | 0.99 | | |
| $(7)^{3,1}\Pi_g$ | $[^2\Pi_g]$ | $0.87\|4d_\sigma\rangle+0.30\|5s\rangle+0.21\|6s\rangle$ | 0.60 | | |
| | $[^2\Pi_u]$ | $0.93\|6p_\sigma\rangle$ | 0.40 | | |
| $(8)^{3,1}\Pi_g$ | $[^2\Sigma_u^+]$ | $0.50\|5f_\pi\rangle$ | 0.98 | | |
| $(9)^{3,1}\Pi_g$ | $[^2\Pi_g]$ | $0.99\|6s\rangle$ | 0.90 | | |
| $(1)^{3,1}\Delta_g$ | $[^2\Sigma_u^+]$ | $0.99\|4f_\delta\rangle$ | 0.99 | | |
| $(2)^{3,1}\Delta_g$ | $[^2\Sigma_u^+]$ | $0.80\|5f_\delta\rangle$ | 0.99 | | |
| $(3)^{3,1}\Delta_g$ | $[^2\Pi_g]$ | $0.94\|4d_\pi\rangle$ | 0.40 | 424 | 344 |
| | $[^2\Pi_u]$ | $0.99\|5p_\pi\rangle$ | 0.60 | | |
| $(4)^{3,1}\Delta_g$ | $[^2\Sigma_u^+]$ | $0.25\|5f_\delta\rangle+0.95\|6f_\delta\rangle$ | 0.99 | | |
| $(5)^{3,1}\Delta_g$ | $[^2\Pi_g]$ | $0.79\|4d_\pi\rangle+0.55\|5d_\pi\rangle$ | 0.60 | 68 | 99 |
| | $[^2\Pi_u]$ | $0.94\|5p_\pi\rangle$ | 0.40 | | |
| $(1)^{3,1}\Sigma_g^-$ | $[^2\Pi_g]$ | $0.94\|5p_\pi\rangle$ | 0.96 | | |

pulsive states namely (6) $^3\Sigma_u^+$ and (7) $^1\Sigma_u^+$ which are both assigned as $[^2\Pi_g]5p_\pi$ and diabatically correlated with the Ar*$(4p)$ dissociation.

In other symmetries, mixings are less important. For instance, the $^{3,1}\Sigma_g^+$ states with $[^2\Sigma_u^+]$ core can be assigned in increasing excitation order as $[^2\Sigma_u^+]5p_\sigma$, $[^2\Sigma_u^+]6p_\sigma$, $[^2\Sigma_u^+]4f_\sigma$, $[^2\Sigma_u^+]7p_\sigma$, $[^2\Sigma_u^+]5f_\sigma$, and $[^2\Sigma_u^+]8p_\sigma$. Those attractive states are crossed by repulsive states originating from Ar*$(4p)$+Ar namely (7) $^{3,1}\Sigma_g^+$ which exhibit $[^2\Pi_u]$ and $[^2\Pi_g]$ mixing and undergo interaction with the next pair of repulsive states namely (10) $^{3,1}\Sigma_g^+$ diabatically correlated in this distance range with the Ar*$(3d)$ dissociation.

In the $^{3,1}\Pi_g$ manifold, $[^2\Sigma_u^+]$ core states are assigned as respectively $[^2\Sigma_u^+]5p_\pi$, $[^2\Sigma_u^+]6p_\pi$, $[^2\Sigma_u^+]4f_\pi$, $[^2\Sigma_u^+]7p_\pi$. The (6) $^{3,1}\Pi_g$ states which have a $[^2\Sigma_u^+]$ core appear as presenting $7p_\pi/5f_\pi$ orbitals mixing. This symmetry also presents repulsive states. The first pair of repulsive states (2) $^{3,1}\Pi_g$ which are correlated with Ar* $(4s)$ have a predominant $[^2\Pi_g]$ core configuration (with $5s$ UAO) whereas the second pair of repulsive states namely (7) $^{3,1}\Pi_g$ correlated with Ar*$(3d)$, present $^2\Pi_g/^2\Pi_u$ core mixing as well as orbital mixing $(0.87[^2\Pi_g]4d_\sigma+0.30[^2\Pi_g]5s+0.21[^2\Pi_g]6s/0.93[^2\Pi_u]6p_\sigma)$.

The attractive $^{3,1}\Pi_u$ states are assigned respectively as $[^2\Sigma_u^+]4d_\pi$, $[^2\Sigma_u^+]5d_\pi$, $[^2\Sigma_u^+]6d_\pi$, $[^2\Sigma_u^+]7d_\pi$. The repulsive $^{3,1}\Pi_u$ states namely (2) $^{3,1}\Pi_u$ and (5) $^{3,1}\Pi_u$ are diabatically correlated with Ar*$(4s)$ and Ar*$(3d)$, respectively.

We now examine the qualitative result of spin–orbit coupling in the $\Omega$ potential curves displayed in Figs. 3(a)–3(h) (their spectroscopic constants are listed in Table III). A first qualitative remark is that at the equilibrium distance of the excimer states, spin–orbit coupling generates numerous quasidegenerate $\Omega$ components but does not generally induce a very strong splitting. In particular, considering intra-Rydberg transitions, the energetical positions of the $\Omega$ components of attractive states with $[^2\Sigma_u^+]$ core are only slightly displaced with respect to the positions of their $\Lambda$–$\Sigma$ parents. Spin–orbit coupling plays a larger qualitative and quantitative role in the intermediate and longer range region $(R>5a_0)$.

Again, as without spin–orbit coupling, the adiabatic $\Omega$ potential curves exhibit two kinds of avoided crossing. The first one concerns interactions between $\Lambda$–$\Sigma$ states in which the main configurations differ by two spinorbitals. In this case, the $\Omega$ potential curve-crossing pattern conserves the same character as for the $\Lambda$–$\Sigma$ parents. Characteristic examples are provided by avoided crossing at $R\sim4.8a_0$ between (2) $0_g^+$ and (3) $0_g^+$, (2) $0_g^-$ and (3) $0_g^-$, (2) $1_g$ and (3) $1_g$, (4) $1_g$ and (5) $1_g$, (1) $2_g$ and (2) $2_g$. This series of avoided crossings follow the weakly avoided crossing between $(1)^{3,1}\Pi_g([^2\Pi_g]\sigma_g^*4s)$ and $(2)^{3,1}\Pi_g([^2\Sigma_u^+]\pi_u^*4p)$ which differ both through the hole and the particle and are correlated with different configurations of the separated atoms. The same kind of situation occurs at short distance $(R=4.8a_0)$ between the repulsive states (2) $0_u^+$, (2) $0_u^-$, (2) $1_u$, (3) $1_u$, and (1) $2_u$ corresponding to $^{3,1}\Pi_u([^2\Pi_u]\sigma_g^*4s)$ parents and the series of $[^2\Sigma_u^+]$ core states correlated to higher asymptotic configurations. The second type of avoidance concerns states which essentially differ through the core only and for which spin–orbit coupling is not vanishing. Such case occurs between (1) $0_g^-$ and (2) $0_g^-$, (1) $0_g^+$ and (2) $0_g^+$ states at $R\sim5.2a_0$. As mentioned previously, the (1) $^{3,1}\Sigma_g^+$ states are mixings of $[^2\Sigma_u^+]\sigma_u^*4p$ and $[^2\Sigma_g^+]\sigma_g^*4s$. The latter configuration interacts via spin–orbit coupling with the repulsive $^{3,1}\Pi_g$ states $([^2\Pi_g]\sigma_g^*4s)$. Another significant example is the avoided crossing between $(1)^1\Sigma_u^+([^2\Sigma_u^+]\sigma_g^*4s)$ and $(1)^1\Pi_u([^2\Pi_u]\sigma_g^*4s)$ which differ through the hole. It induces a well at $R\sim6.8a_0$ for the (2) $0_u^+$ state. This is a case of intermediate distance spin–orbit avoided crossing between $\Lambda$-$\Sigma$ states correlated with the same configuration of the separated atoms. Another similar case occurs at $R\sim6.5a_0$ in the gerade manifolds $0_g^-$ and $1_g$. It involves the interaction of (2) $^{3,1}\Pi_g([^2\Sigma_u^+]\pi_u^*4p)$ and (3) $^3\Sigma_g^+$ via the weight of the $[^2\Pi_u]\pi_u^*4p$ configuration contributing in the latter.

The underlying $\Lambda$–$\Sigma$ parents in the $\Omega$ states of ungerade symmetry at $R=4.6a_0$ are (1) $^3\Sigma_u^+$, (2) $^3\Sigma_u^+$, (1) $^3\Pi_u$, (1) $^1\Pi_u$, and (3) $^3\Sigma_u^+$ in the $0_u^-$ manifold, (1) $^1\Sigma_u^+$, (2) $^1\Sigma_u^+$, (1) $^3\Pi_u$, (1) $^1\Pi_u$ and (3) $^1\Sigma_u^+$ in the $0_u^+$ manifold, (1) $^3\Sigma_u^+$, (2) $^3\Sigma_u^+$, (1) $^3\Delta_u$, (1) $^3\Pi_u$, (1) $^1\Pi_u$, (3) $^3\Sigma_u^+$ in the $1_u$ manifold, (1) $^3\Delta_u$, (1) $^3\Pi_u$, (2) $^3\Pi_u$, and (2) $^3\Delta_u$ for $\Omega=2$ and (1) $^3\Delta_u$ for $\Omega=3$.

For the gerade manifold, at $R=4.6a_0$, the $\Lambda$-$\Sigma$ content of the $\Omega$ states is assigned in the labeling of the $\Omega$ states of Table III.

## III. COMPARISON WITH PREVIOUS THEORETICAL RESULTS

Several *ab initio* calculations are available in the literature concerning more or less extensive parts of the excited spectrum of the $Ar_2^*$ excimer. The first quantitative calculations were achieved by Saxon and Liu[3] on the $^3\Sigma_u^+$ and $^3\Sigma_g^+$ lowest triplet states dissociating into Ar*$(4s)$+Ar with an all-electron frozen core approach involving MCSCF and CI treatment without spin–orbit coupling. Subsequent calculations concerned with all the states correlated with the Ar*$(4s)$+Ar asymptote took advantage of the effective core or pseudopotential techniques. One may quote the work of Castex *et al.*[6] using pseudopotentials and variational/perturbative multireference CI. Later, Yates *et al.*[10] treated the same states with the effective core potential formalism using first-order polarization CI (POL-CI). More recently, Mizukami and Nakatsuji[15] published all-electron results for this configuration with symmetry-adapted configuration interaction technique (SAC-CI). In all those studies, spin–orbit coupling was incorporated using the atoms-in-molecules semiempirical technique introduced by Cohen and Schneider.[1] One should be aware that applying the Cohen and Schneider scheme abruptly to the adiabatic states originating from the $4s$ configuration using the asymptotic $3p^5 4s$ coupling scheme and parametrization should break down in regions where the adiabatic states encounter strong configuration mixings or avoided crossings with higher configurations. In particular, the lowest (1) $^{1,3}\Sigma_g^+$ states which transform slowly from $[^2\Sigma_g^+]$ core to $[^2\Sigma_u^+]$ core and from $4s$

(SAO limit) excitation to $5p$ (UAO limit), as well as the lowest adiabatic $(1)^{3,1}\Pi_g$ states with $[^2\Pi_g]$ core which undergo weakly avoided crossings with the upper $(2)^{3,1}\Pi_g$ core states having $[^2\Sigma_u^+]$ core should not be straightfully treated in the Cohen and Schneider scheme, unless the treatment is applied in a diabatic representation, at least for the hole. As concerns states dissociating toward higher asymptotes, one may mention the work of Gadea and Spiegelmann[7] without spin–orbit coupling, who extended the work of Castex *et al.*[6] to states dissociating into Ar*$(4p)$+Ar and their adiabatic interaction with higher configurations. More recently, partial results can be found in the work of Mizukami and Nakatsuji.[15] Finally, one should quote the work of Teichteil and Spiegelmann[11] where *ab initio* spin–orbit pseudopotential techniques coupled with variational/perturbative MRCI were used in order to determine all the gerade adiabatic states dissociating into Ar*$(4s)$+Ar and Ar*$(4p)$+Ar.

Before undertaking a state by state discussion, we compare the two methods used for dealing with two electron integrals in the present work, focusing on the exchange inte-

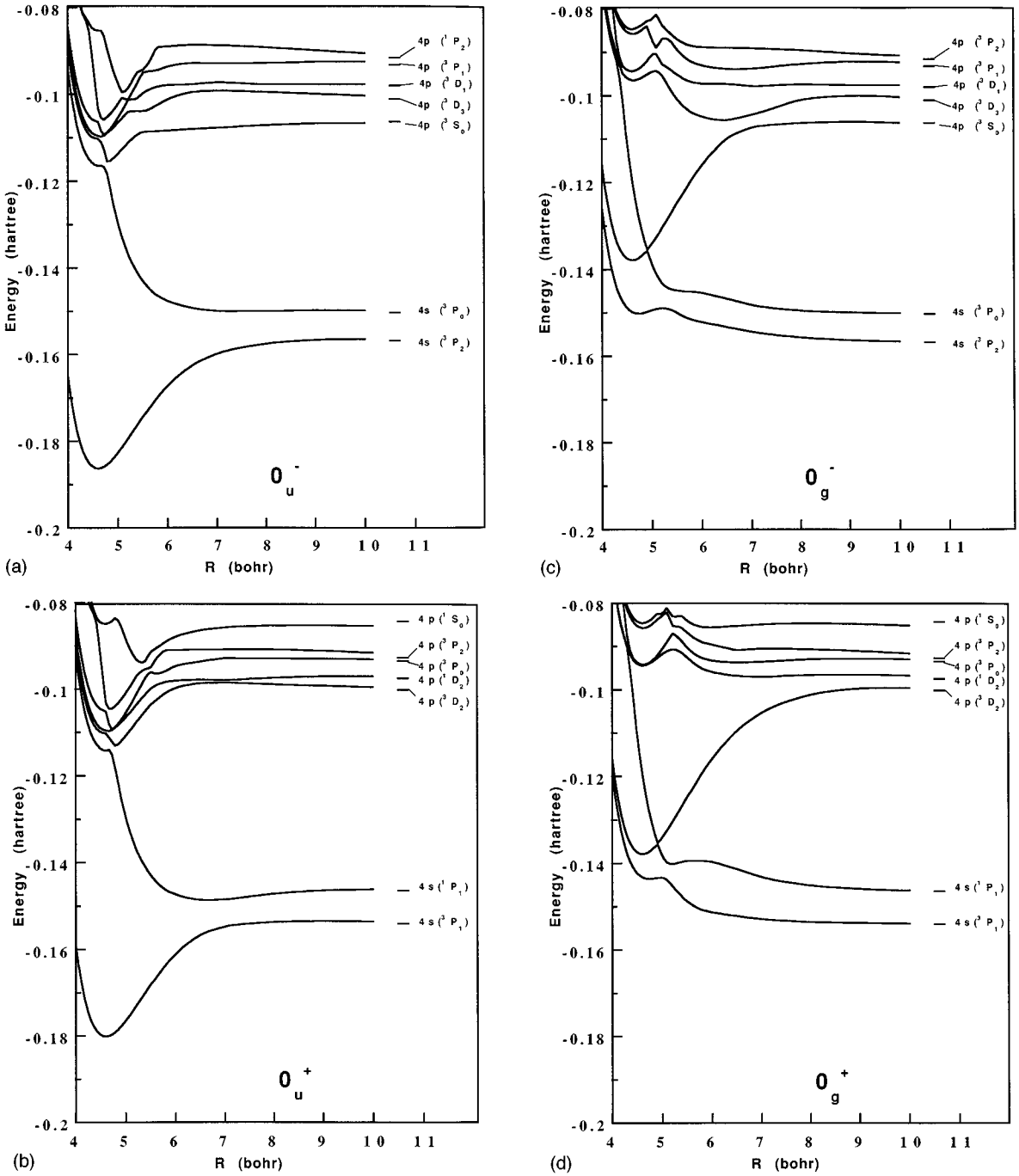


FIG. 3. Potential energy curves of the excited states of $Ar_2^*$ with spin–orbit coupling. (a) $0_u^-$, states; (b) $0_u^+$ states; (c) $0_g^+$ states; (d) $0_g^+$ states; (e) $1_g$ states; (f) $1_u$ states; (g) $2_u$ states (full lines) and $3_u$ states (dotted lines); (h) $2_g$ states (full lines) and $3_g$ states (dotted lines).

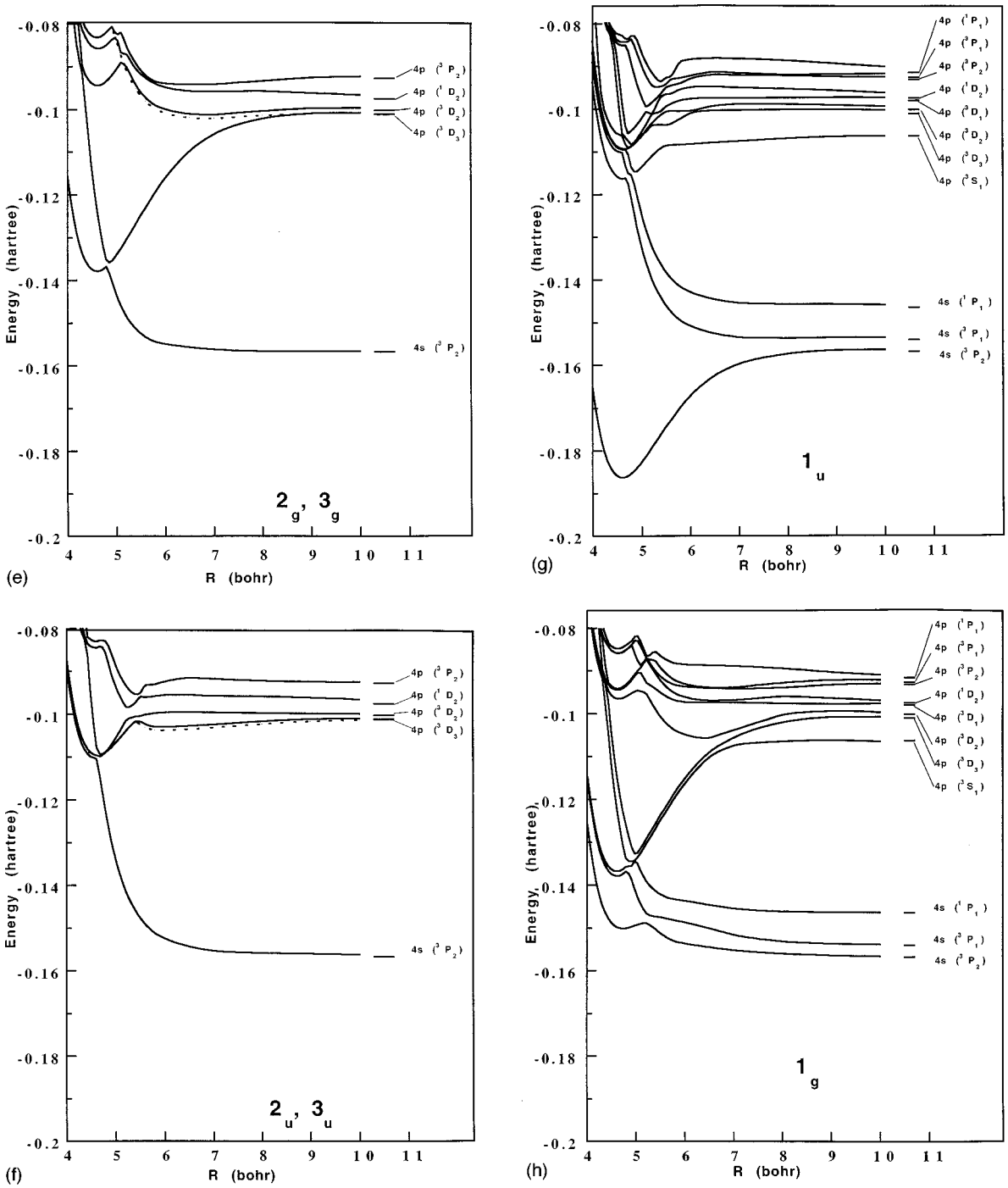


FIG. 3. (*Continued.*)

grals governing the singlet–triplet separation $\Delta_{ST}$ at short internuclear distance ($R=4.6a_0$). This separation is shown in Table II according to the method using the overlaps of the molecular orbitals with atomic orbitals (method *A*) and the operatorial scheme (method *B*). Generally, method *A* yields singlet–triplet separation larger than method *B*. Due to the physical natural decrease of this quantity when one goes to higher excitations in the Rydberg spectrum, the largest differences obviously concern the states diabatically correlated with the lowest atomic configuration Ar*(4s)+Ar. For instance for the lowest $^{1,3}\Sigma_u^+$ excimer state, method *A* yields $\Delta_{ST}=1349$ cm$^{-1}$, close to the atomic value $\Delta_{ST}=1440$ cm$^{-1}$, whereas method *B* yields $\Delta_{ST}=870$ cm$^{-1}$ a much lower value. Unfortunately, both values remain in the range provided by *ab initio* calculations, e.g., $\Delta_{ST}=790$ cm$^{-1}$ (Castex *et al.*),[6] 870 cm$^{-1}$ (Spiegelmann and Gadea[8]), 1314 cm$^{-1}$ (Yates *et al.*[10]), ~1000 cm$^{-1}$ (Mizukami and Nakatsuji[15]). This is also the range of the experimental dispersion.[19–21] Similarly for the two lowest gerade $^{1,3}\Sigma_g^+$, method *A* provides a value of 1454 cm$^{-1}$, again close to the atomic limit,

TABLE III. Spectroscopic constants of the $\Omega$ states of $Ar_2^*$.

| States | $R_e$ (Å) | $T_e$ ($cm^{-1}$) | $\omega_e$ ($cm^{-1}$) | $\omega_e x_e$ ($cm^{-1}$) | $B_e$ ($cm^{-1}$) |
|---|---|---|---|---|---|
| $(1)0u^-((1)^3\Sigma_u^+)$ | 2.435 | | 296 | 2.783 | 0.1424 |
| $(1)1u((1)^3\Sigma_u^+)$ | 2.435 | 1 | 296 | 2.789 | 0.1424 |
| $(1)0u^+((1)^1\Sigma_u^+)$ | 2.434 | 1347 | 296 | 2.774 | 0.1425 |
| $(1)0g^-((1)^3\Sigma_g^+)$ | 2.503 | 7927 | 207 | 27.5 | 0.1344 |
| $(1)1g((1)^3\Sigma_g^+)$ | 2.502 | 7928 | 210 | 25.0 | 0.1346 |
| $(1)0g^+((1)^1\Sigma_g^+)$ | 2.366 | 9453 | 188 | 49.2 | 0.1336 |
| $(2)0g^+((1)^3\Pi_g)$ | 2.437 | 10629 | 302 | 2.326 | 0.1422 |
| $(2)0g^-((1)^3\Pi_g)$ | 2.437 | 10627 | 303 | 2.477 | 0.1422 |
| $(2)1g((1)^3\Pi_g)$ | 2.437 | 10627 | 303 | 2.675 | 0.1421 |
| $(1)2g((1)^3\Pi_g)$ | 2.437 | 10626 | 302 | 2.346 | 0.1422 |
| $(3)1g((1)^1\Pi_g)$ | 2.436 | 10867 | 303 | 2.345 | 0.1422 |
| $(4)0g^-((2)^3\Sigma_g^+)$ | 2.454 | 19724 | 278 | 10.86 | 0.1400 |
| $(6)1g((2)^3\Sigma_g^+)$ | 2.453 | 19725 | 285 | 10.99 | 0.1402 |
| $(5)0g^+((3)^3\Pi_g)$ | 2.448 | 20872 | 297 | 2.80 | 0.1408 |
| $(5)0g^-((3)^3\Pi_g)$ | 2.433 | 20161 | 306 | 10.48 | 0.1425 |
| $(7)1g((3)^3\Pi_g)$ | 2.438 | 20161 | 305 | 4.46 | 0.1419 |
| $(3)2g((3)^3\Pi_g)$ | 2.444 | 20162 | 305 | 4.46 | 0.1419 |
| $(1)3g((3)^3\Pi_g)$ | 2.430 | 22628 | 311 | 4.25 | 0.1428 |
| $(4)0g^+((2)^1\Sigma_g^+)$ | 2.438 | 20160 | 293 | 10.42 | 0.1419 |
| $(8)1g((3)^1\Pi_g)$ | 2.444 | 20232 | 305 | 4.48 | 0.1419 |
| $(6)0g^+((4)^3\Pi_g)$ | 2.444 | 22058 | 297 | 5.21 | 0.1412 |
| $(6)0g^-((4)^3\Pi_g)$ | 2.444 | 22058 | 297 | 5.31 | 0.1412 |
| $(9)1g((4)^3\Pi_g)$ | 2.444 | 22058 | 297 | 5.25 | 0.1412 |
| $(4)2g((4)^3\Pi_g)$ | 2.444 | 22058 | 305 | 5.21 | 0.1412 |
| $(10)1g((4)^1\Pi_g)$ | 2.444 | 22062 | 297 | 5.18 | 0.1412 |
| $(7)0g^-((3)^3\Sigma_g^+)$ | 2.434 | 22292 | 298 | 12.8 | 0.1423 |
| $(11)1g((3)^3\Sigma_g^+)$ | 2.439 | 22292 | 297 | 5.86 | 0.1418 |
| $(7)0g^+((3)^1\Sigma_g^+)$ | 2.438 | 22309 | 301 | 5.13 | 0.1420 |
| $(5)2g((1)^3\Delta_g)$ | 2.430 | 22628 | 311 | 4.25 | 0.1428 |

whereas method *B* yields a value of 976 $cm^{-1}$. The range of existing calculations provide 1126 $cm^{-1}$ (Castex *et al.*), 1326 $cm^{-1}$ (Gadea and Spiegelmann), ~1600 $cm^{-1}$ (Yates *et al.*), ~1000 $cm^{-1}$ (Mizukami and Nakatsuji). Thus it is not possible to decide from the literature which method is preferable. One may think that the two methods provide upper and lower bounds to the singlet–triplet splitting. We remind that potential curves without and with spin–orbit coupling have been derived using method *A*, although we often also quote in the discussion results involving method *B* for sake of comparison and completeness. The agreement between the two methods is better for the (2) $^{3,1}\Pi_g$ states at $R=4.6a_0$, diabatically repulsive and correlated with Ar*(4*s*)+Ar (1375 $cm^{-1}$ with method *A*, 1091 $cm^{-1}$ with method *B*) and for the (2) $^{3,1}\Pi_u$ states (1297 and 1198 $cm^{-1}$, respectively). For the higher excited states, the singlet–triplet splitting found with both methods becomes smaller but generally falls in the order of magnitude of the available *ab initio* values of Spiegelman and Gadea.[8]

We now examine the two lowest excimer states $^{3,1}\Sigma_u^+$. The $R_e$, $D_e$, and $\omega_e$ values are compared with those obtained in previous *ab initio* calculations without spin–orbit coupling. One may remark that the equilibrium distances for the two states, respectively $R_e=2.434$ Å and $R_e=2.433$ Å are slightly larger than the one obtained for the $\Lambda$–$\Sigma$ parent ion state $^2\Sigma_u^+$[$R_e=2.425$ Å, $D_e=11\,225$ $cm^{-1}$ (1.39 eV), $\omega_e=314$ $cm^{-1}$, $\omega_e x_e=2.115$ $cm^{-1}$ without spin–orbit coupling]. This effect is expected, due to the partial screening of the extra Rydberg electron. Simultaneously, the dissociation energies are also reduced with respect to the ion, respectively $D_e=6928$ $cm^{-1}$ (0.859 eV) for the triplet state, and $D_e=7019$ $cm^{-1}$ (0.870 eV) for the singlet state. If method *B* is used, those value are changed by about 300 $cm^{-1}$ and become 6633 $cm^{-1}$ (0.822 eV) and 7313 $cm^{-1}$ (0.906 eV) respectively. The equilibrium distances found here are at the low limit of those found in the *ab initio* CI calculations (in the range 2.43–2.47 Å) and the dissociation energies are larger (0.68 eV in the work of Saxon and Liu,[3] 0.706 eV in the work of Spiegelmann and Gadea,[8] 0.550 eV in the work of Yates *et al.*[10] and ~0.50 eV in the work of Mizukami and Nakatsuji[15] for the $^3\Sigma_u^+$ state, 0.773,[8] 0.596,[10] and 0.56 eV,[15] respectively for the $^1\Sigma_u^+$ state). This is understandable since we work with more attractive contributions due to the use of core data closer to experiment, whereas the *ab initio* calculations of $Ar_2^+$ consistent with those of $Ar_2^*$ usually underestimate the ion binding energy (without spin–orbit coupling 1.27 eV in the work of Spiegelmann,[22] 1.28 eV in the work of Christiansen *et al.*[9] in close agreement with the all-electron frozen core calculation of Wadt,[4] ~1.20 eV in the work of Mizukami and Nakatsuji[15]). This is due to the difficulty of correlating the 15 remaining explicit electrons involved in the valence MOs. Accordingly to the obtention of more strongly bound states, $\omega_e$ constants for the two lowest excimer states ($\omega_e=294$ $cm^{-1}$) are larger than those found in *ab initio* CI calculations. When spin–orbit coupling is in-

TABLE IV. Detailed features of the (1) $^2\Sigma_g^+$ and $(1)^1\Sigma_g^+$ states. $R_e$ and $R_m$ are the distances corresponding to equilibrium and the barrier maximum, $V_e$ and $V_m$ are the corresponding energy values with respect to the respective asymptotes $^3P$ and $^1P$. $\Delta$ corresponds to the depth of the minimum below the barrier.

| | | $R_e$ (bohr) | $R_m$ (bohr) | $V_e$ ($cm^{-1}$) | $V_m$ ($cm^{-1}$) | $\Delta$ ($cm^{-1}$) |
|---|---|---|---|---|---|---|
| $(1)^3\Sigma_g^+$ | This work | 4.71 | 5.60 | 1013 | 1747 | 734 |
| | Saxon *et al.* (Ref. 3) | 4.76 | 5.87 | 853 | 1913 | 1060 |
| | Spiegelmann *et al.* (Ref. 8) | 4.84 | 5.57 | 1750 | 2108 | 359 |
| | Yates *et al.* (Ref. 10) | 4.68 | 5.71 | 1613 | 2097 | 484 |
| $(1)^1\Sigma_g^+$ | This work | 4.71 | 5.60 | 1027 | 1760 | 733 |
| | Spiegelmann *et al.* (Ref. 8) | 4.78 | 5.67 | 1681 | 2281 | 600 |
| | Yates *et al.* (Ref. 10) | 4.83 | 5.73 | 1710 | 2290 | 580 |

cluded, the dissociation energies of the $1_u$, $0_u^-((1)^3\Sigma_u^+)$ and $0_u^+(1)^1\Sigma_u^+$ are reduced to 6474 $cm^{-1}$(0.80 eV) and 5733 $cm^{-1}$ (0.71 eV), the other spectroscopic constants being weakly affected by spin–orbit. This is accordingly larger than the values found by the previous authors (in the range of 0.45–0.68 eV).

The lowest gerade $^{3,1}\Sigma_g^+$ states are particularly sensitive since, as already discussed they present a relative well followed by a barrier to dissociation. The results for those two states and the available *ab initio* results are summarized in Table IV. Concerning the barrier height and the relative depth of the minimum with respect to the top of the barrier, our calculations provide intermediate values (734 $cm^{-1}$ for the triplet, 733 $cm^{-1}$ for the singlet) between those of the all-electron frozen-core calculations of Saxon and Liu[3] and those of the pseudopotential or effective core potential calculations (the two latter methods yielding very similar results). Surprisingly, Mizukami and Nakatsuji[15] found no minima for those two curves, obtaining essentially repulsive states with marked shoulders in the short distance range. One should notice that the equilibrium distances ($R_e=4.71$ $a_0$ in the present work) are displaced toward larger values with respect to those of the lowest ungerade states ($R_e=4.60$ $a_0$ for both triplet and singlet states). This is also the trend observed in the *ab initio* calculations as reported in Table IV. Simultaneously, the $\omega_e$ constants ($\omega_e\sim226$ $cm^{-1}$) are smaller than those of the $^{3,1}\Sigma_u^+$ states and the anharmonicity is larger. Those quantitative differences are clearly due to the slow transformation affecting the lowest excited gerade states when the distance is increased and the progressive switching from attractive core to repulsive core. An interesting issue when spin–orbit coupling is included in the present results is that $(1)1_g$, $0_g^-$, and $(1)0_g^+$ keep a bound nature with respect to the barrier maximum, which was not the case of previous studies involving spin–orbit coupling. Due to the spin–orbit interaction, however, the $\omega_e$ constants are slightly reduced with comparison to those of their $\Lambda$–$\Sigma$ parents.

The next strongly bound states in the short distance range are states $(1)^{3,1}\Pi_g$ which are diabatically correlated with the $4p$ separated atom limits $^3D$ and $^1D$. Their dissociation energies with respect to these diabatic asymptotes are in our calculations 8508 $cm^{-1}$ (1.055 eV) for the triplet and 8767 $cm^{-1}$ (1.087 eV) for the singlet state. Those values are in good agreement with those obtained in the *ab initio* calculations of Spiegelmann and Gadea (1.007 eV for the triplet, 0.955 eV for the singlet) but larger than the values obtained by Mizukami and Nakatsuji (~0.77 eV for the two states).

A fewer higher states were studied in the work of Spiegelmann and Gadea,[8] namely $(2)^{3,1}\Sigma_g^+$, (2) and $(3)^{3,1}\Sigma_u^+$, $(3)^{3,1}\Pi_g$, (1) and $(3)^{3,1}\Pi_u$, and $^{3,1}\Delta_u$. The present transitions energies $T_e$ (see Table I) for those states, calculated above the minimum of the lowest excimer state $(1)^3\Sigma_u^+$ are in reasonable good agreement with the *ab initio* values which are generally smaller by 500–600 $cm^{-1}$.

As mentioned earlier, spin–orbit coupling does not alter significantly the spectroscopic constants of the states in the short distance range, except for the lowest ones. Those for the gerade $\Omega$ states are listed in Table III. Those for the ungerade states which are predissociated in the neighborhood of their minima, can be identified with those of their $\Lambda$–$\Sigma$ parents.

Tables I and III also provide the evolution of the spectroscopic constants for the Rydberg states of various symmetries with increasing excitation. One can see rather clearly the general trend, namely the convergency toward the $Ar_2^+$ values for the equilibrium distances within the accuracy obtained in determining those constants. This convergency is not always quite monotonic, due to the fact that a given total $\Lambda$–$\Sigma$ molecular symmetry can involve several Rydberg series with different united atom orbitals such as even $ns$ or $nd$ orbitals for the ungerade states or $np$ and $nf$ for the gerade states (the underlying attractive $[^2\Sigma_u^+]$ core always has ungerade symmetry).

## IV. COMPARISON WITH EXPERIMENT

Two essential types of absorption have been observed and rather extensively studied in excimers. The first one concerns absorption from the ground state and involves upper states of ungerade symmetry in the distance range around the equilibrium distance of the ground state $R_e=3.59$ Å, namely $(1)1_u$, $(1)0_u^+$, and $(2)0_u^+$ states. The second type concerns intra-Rydberg transitions, they consist in first populating the quasidegenerate $(1)1_u$, $0_u^-$ states and then observing absorption from those excited states.

Information for the $(1)1_u$, $0_u^-$ states is available from both of those experiments, absorption from the ground state

TABLE V. Vibrational levels of the (1) $1u$, (1) $0u^+$, and (2) $0u^+$ states. The experimental results correspond to Ref. 24.

| | Experimental ($cm^{-1}$) | | | | This work ($cm^{-1}$) | | | |
|---|---|---|---|---|---|---|---|---|
| Level $v'$ | $G_v$ | $\Delta G_v$ | $R_{in}$ (bohr) | $R_{out}$ (bohr) | $G_v$ | $\Delta G_v$ | $R_{in}$ (bohr) | $R_{out}$ (bohr) |
| (1) $1_u$ | | | | | | | | |
| 20 | | | | | 4824 | | 3.993 | 6.270 |
| 21 | | | | | 4990 | 166 | 3.985 | 6.354 |
| 22 | | | | | 5149 | 159 | 3.979 | 6.443 |
| 23 | 4943.9 | | 3.916 | 6.546 | 5300 | 151 | 3.973 | 6.537 |
| 24 | 5081.9 | 138.0 | 3.904 | 6.644 | 5443 | 143 | 3.968 | 6.638 |
| 25 | 5210.3 | 128.4 | 3.892 | 6.755 | 5578 | 135 | 3.966 | 6.745 |
| 26 | 5328.6 | 118.3 | 3.883 | 6.884 | 5704 | 126 | 3.960 | 6.860 |
| 27 | 5436.0 | 107.4 | 3.874 | 7.031 | 5822 | 118 | 3.956 | 6.984 |
| 28 | 5531.9 | 95.9 | 3.866 | 7.207 | 5932 | 108 | 3.953 | 7.118 |
| 29 | 5614.2 | 82.3 | 3.856 | 7.428 | 6030 | 100 | 3.950 | 7.264 |
| 30 | 5681.0 | 66.8 | 3.855 | 7.685 | 6122 | 92 | 3.947 | 7.424 |
| 31 | | | | | 6205 | 83 | 3.945 | 7.597 |
| (1) $0_u^+$ | | | | | | | | |
| 20 | 4575.8 | | 3.909 | 6.200 | 4839 | | 3.992 | 6.304 |
| 21 | 4742.5 | 166.7 | 3.900 | 6.283 | 5002 | 163 | 3.984 | 6.373 |
| 22 | 4900.0 | 157.5 | 3.891 | 6.377 | 5156 | 154 | 3.978 | 6.507 |
| 23 | 5047.7 | 147.7 | 3.881 | 6.482 | 5297 | 141 | 3.973 | 6.628 |
| 24 | 5184.3 | 136.6 | 3.874 | 6.600 | 5425 | 128 | 3.968 | 6.771 |
| 25 | 5308.2 | 123.9 | 3.864 | 6.740 | 5537 | 112 | 3.965 | 6.943 |
| 26 | 5417.4 | 109.2 | 3.855 | 6.918 | 5632 | 95 | 3.961 | 7.147 |
| 27 | 5508.0 | 90.6 | 3.855 | 7.116 | 5711 | 79 | 3.959 | 7.394 |
| (2) $0_u^+$ | | | | | | | | |
| 0 | 32.4 | | 6.527 | 7.143 | 37 | | 6.429 | 6.996 |
| 1 | 91.2 | 58.8 | 6.361 | 7.489 | 109 | 72 | 6.256 | 7.291 |
| 2 | 142.1 | 50.9 | 6.268 | 7.819 | 176 | 67 | 6.146 | 7.517 |
| 3 | 184.9 | 42.6 | 6.222 | 8.199 | 239 | 63 | 6.061 | 7.721 |
| 4 | 219.8 | 34.9 | 6.183 | 8.609 | 297 | 58 | 5.993 | 7.915 |
| 5 | 248.1 | 28.3 | 6.141 | 9.032 | 351 | 54 | 5.937 | 8.116 |
| 6 | 272.2 | 24.1 | 6.141 | 9.486 | 401 | 50 | 5.892 | 8.333 |
| 7 | 292.4 | 20.2 | 6.141 | 9.958 | 446 | 45 | 5.855 | 8.576 |
| 8 | 310.7 | 18.3 | 6.160 | 10.431 | 487 | 41 | 5.826 | 9.867 |
| 9 | 327.1 | 16.4 | 6.179 | 11.017 | | | | |

characterizing high vibrational levels, whereas transient absorption provides reliable information about the low vibrational levels. After the pioneering experimental work of Tanaka and Yoshino[23] who observed nine band systems from the ground state, Herman *et al.*[24,25] recently performed high resolution analysis of the VUV absorption. They observed vibrational levels in the range $v'=23$–$30$ and estimated from linear extrapolation the maximum number of vibrational levels to be $v'_{max}=34$. They observed no obvious hint for the presence of a possible hump at long distance, as discussed for other systems such as $Ne_2^*$ for instance, and occurring in some of the *ab initio* calculations.[1,12] Although extrapolation to the lowest vibrational levels is far from being very accurate and does not allow for the determination of the spectroscopic constants, they gave an estimation of $5786\pm500$ $cm^{-1}$ ($0.72$ eV$\pm0.06$) for the dissociation energy using theoretical values for $B_e$ ($0.14$ $cm^{-1}$) taken from Castex *et al.*[6] and $\omega_e$($265.5$ $cm^{-1}$) taken from Yates *et al.*[10] From rainbow scattering experiments, Gillen *et al.*[26] had estimated $D_e$ to be 0.78 eV. From the recent determination of the ionization threshold $29\,373$ $cm^-$,[27] and considering the experimental value for the dissociation energy of the $Ar_2^+$ ground state, the atomic ionization threshold $34\,066.1$ $cm^{-1}$, and the difference in the $\omega_e$ constants ($314$ $cm^{-1}$ for $Ar_2^+$, $296$ $cm^{-1}$ for $Ar_2$) one can get a rather reliable determination for $D_e$ of $6034$ $cm^{-1}$ ($0.75$ eV) in rather good correspondence with the previous experimental values. The present theoretical value is $6473$ $cm^{-1}$ ($0.80$ eV), slightly larger (this value corresponds to the use of method A for the two electrons integrals; the value is reduced to 0.76 eV with method B). The vibrational constants $\omega_e=296$ $cm^{-1}$ and $\omega_e x_e=2.79$ $cm^{-1}$ are in excellent agreement with the work of Kane *et al.* ($\omega_e=296$ $cm^{-1}$, $\omega_e x_e=2.79$ $cm^{-1}$). The present potential curve exhibits a very small hump of $85$ $cm^{-1}$ above the dissociation limit at $R\approx10a_0$. Using a Numerov integration method, we have determined that this electronic state accepts 31 vibrational levels as far as only bound states are considered, but it might accept three quasibound states between the dissociation limit and the hump maximum. The number of calculated bound vibrational levels is in very good concordance with the work of Herman *et al.*[25] Table V shows the comparison of the present theoretical vibrational energies

and spacings in the range $v'=23$–$30$ with the experimental values of Herman *et al.*,[25] together with the rotational constants and the turning points $R_{\text{in}}$ and $R_{\text{out}}$. Information about this state is also available in emission fluorescence.[28–31] As seen from the agreement between calculated $\Delta G_v$ spacings, $R_{\text{in}}$ and $R_{\text{out}}$ values and experimental values, the discrepancy as concerns vibrational numbering is at most one unit. The calculated $R_{\text{in}}$ values are slightly longer than the experimental ones. However, the ambiguities about the precise knowledge of the repulsive shape of the ground state and the lack of direct experimental evidence about the equilibrium distance preclude from achieving accurate estimation of $D_e$ through these experiments.

There are no transient absorption data available for the $(1)0_u^+$ state due to its short lifetime. An experimental value for $D_e$ was found from emission measurements[32] ($6000\pm600$ $\text{cm}^{-1}$). As for the very parallel $1_u$, $0_u^-$ states, observing the vibrational levels in the range $v'=20$–$27$, Herman *et al.*[25] gave an estimation $D_e=5640\pm400$ $\text{cm}^{-1}$ (0.711 eV), very close to their dissociation energy of the $1_u$, $0_u^-$ states. The value presently calculated is $D_e=5733$ $\text{cm}^{-1}$ (0.710 eV) and raises up to 6033 $\text{cm}^{-1}$ if integral method *B* is used. Herman *et al.* found levels up to $v'=27$ for those states, in agreement with our theoretical numbering (Table V). Our $(1)0_u^+$ state also has a small barrier above the dissociation of about 68 $\text{cm}^{-1}$ at $R\sim9$ $a_0$. The accuracy for the long range behavior in the present work is certainly limited, in particular due to the neglect of two-electron interatomic resonance integrals which might cause the present hump to disappear (attractive $-2C_3/R^3$ contributions). Such a small barrier was invoked by Tanaka *et al.*[22] to explain the very diffuse character of the absorption bands corresponding to the last vibrational levels. The calculated properties of the vibrational levels for this electronic state are summarized in Table V. There is again an overall agreement within one vibrational unit between calculated and experimental values.

The next state $(2)0_u^+$ has its equilibrium distance closer to the ground state bound region, since its minimum is the adiabatic consequence of a spin–orbit avoided coupling between the repulsive $^3\Pi_u$ state and the attractive $^1\Sigma_u^+$ state in the medium distance range. The lowest vibrational levels ($v'=0$–$9$) could thus be observed experimentally and the vibrational constants were determined with better accuracy. In general agreement with the previous work of Tanaka *et al.*,[33] Herman *et al.*[25] proposed $R_e=3.596$ Å, $D_e=465.8$ $\text{cm}^{-1}$, $\omega_e=68.16$ $\text{cm}^{-1}$, and $\omega_e x_e=4.631$ $\text{cm}^{-1}$. The present values $R_e=3.542$ Å, $D_e=488.7$ $\text{cm}^{-1}$, $\omega_e=75$ $\text{cm}^{-1}$, $\omega_e x_e=1.713$ $\text{cm}^{-1}$ are in satisfactory agreement with the experimental ones. One should notice however that the harmonic constant is slightly larger than the experimental value, whereas the anharmonic contribution $\omega_e x_e$ is smaller, which results in a divergency between calculated and experimental vibrational levels for $v'>4$. A possible reason might be a lesser of accuracy in this medium distance range of the $Ar_2^+$ $[^2\Sigma_u^+]$ or $[^2\Pi_u]$ core inputs underlying the $^1\Sigma_u^+$ and $^3\Pi_u$ states.

The rest of the experimental spectroscopic information concerns transient absorption from the first vibrational levels of the metastable $(1)1_u$, $0_u^-$ states with $^3\Sigma_u^+$ parent to upper excited states of gerade symmetry.[27,34–42] Early studies concerned the infrared absorption.[34–36] First, Arai *et al.*[35] reported two absorption band systems. The first group has three bands at 10 417 $\text{cm}^{-1}$ (1.292 eV), 10 252 $\text{cm}^{-1}$ (1.271 eV), and 10 118 $\text{cm}^{-1}$ (1.255 eV), and the upper states were assigned by them as belonging to $\Omega$ components of the $(1)^3\Pi_g$ configuration diabatically originating from the 4*p* dissociation. Further experimental studies by Kasama *et al.*[36] maintained the original assignment and resolved the structure of the most intense peak (10 118 $\text{cm}^{-1}$) into four components within an energy range of 35 $\text{cm}^{-1}$. Finding no strong temperature dependence for the those components, they favored the hypothesis of fine structure splitting of the upper state rather than temperature-dependant vibrational population of the lower state. The likeness of the $(1)^3\Sigma_u^+\rightarrow(1)^3\Pi_g$ assignment was also demonstrated by subsequent CI calculations involving *ab initio* averaged and spin–orbit pseudopotentials [9910 $\text{cm}^{-1}$ for the $(1)1_u$, $0_u^-\rightarrow(1)1_g$ transition in the work of Teichteil *et al.*[11]]. In more recent experimental studies,[27] this transition was considered as the first member of the $(1)1_u$, $0_u^-\rightarrow np\ ^3\Pi_g$ Rydberg series. In fact, the triplet and the singlet states $(1)^{3,1}\Pi_g$ are very close together, and one may wonder about possible spin–orbit mixing. In the present work, the $T_e$ values toward $(1)^{3,1}\Pi_g$ states $\Omega$ components are 10 627 $\text{cm}^{-1}$ ($(2)1_g$, (2) $0_g^-$, $(2)0_g^+$, and $(1)2_g$) and 10 867 $\text{cm}^{-1}$, ($(3)1_g$). When using method *B* those values become 10 360 $\text{cm}^{-1}$ and 10 493 $\text{cm}^{-1}$. It has to be noticed that since the Rydberg electron spin–orbit coupling is not involved in the present model, we obtain here vanishing fine structure splitting for those states which have the same core component. In the *ab initio* work of Teichteil *et al.*,[11] the fine structure $^3\Pi_g$ splitting was anyway found to be as small as 21 $\text{cm}^{-1}$ (of the same magnitude as the experimental 26 $\text{cm}^{-1}$ 4*p* atomic fine structure constant), whereas the $(2)1_g$–$(3)1_g$ (triplet–singlet) separation was 136 $\text{cm}^{-1}$, to be compared with 241 $\text{cm}^{-1}$ (method *A*) and 133 $\text{cm}^{-1}$ (method *B*) according to the present model. One may also remark that experimentally, the first and last band maxima at 10 118 and 10 417 $\text{cm}^{-1}$ in the work of Arai *et al.*[35] are separated by exactly 299 $\text{cm}^{-1}$, which is very close to both the initial state [$(1)1_u$, $0_u^-$: $\omega_e=296$ $\text{cm}^{-1}$] and final state ($\omega_e\sim303$ $\text{cm}^{-1}$) vibrational constants. Thus a possible interpretation for the 10 417 $\text{cm}^{-1}$ peak is the occurrence of $v''=0\rightarrow v'=1$ vibrational transition. Finally, the intermediate peak of Arai *et al.* at 10 252 $\text{cm}^{-1}$ may from an energetical point of view correspond to a transition towards state $(3)1_g$, although the $^1\Pi_g$–$^3\Pi_g$ spin–orbit mixing is expected to be weak if one considers the expected magnitude of the SO constant versus the singlet–triplet separation ($\Delta_{\text{ST}}$). Although the present interpretation seems consistent from an energetical point of view, one should remain prudent, due to the crossing of those $^{3,1}\Pi_g$ states by repulsive states of same symmetry diabatically correlated with the 4*s* atomic states [Figs. 1(e) and 1(f)]. This very weakly avoided crossing occurs at $R=4.9$ $a_0$ and $\sim585$ $\text{cm}^{-1}$ above the diabatic minimum of the $(2)0_g^-$ ($^3\Pi_g$) state which therefore contains two unperturbed bound states below the crossing point.

In the $1_g$ manifold, both $^1\Pi_g$ and $^3\Pi_g$ states are predissociated by the lowest repulsive state $^3\Pi_g$ and the level $v'=1$ of $^1\Pi_g$ should be strongly predissociated.

The second group of Arai *et al.*[35] shows two narrow peaks situated at lower transition energies 7899 $cm^{-1}$ (0.979 eV) and 8078 $cm^{-1}$ (1.001 eV) followed by other structures at 8258, 8350, and 8410 $cm^{-1}$. This was initially tentatively attributed by Arai *et al.*[35] as due to transitions from state $(1)0_u^+$ toward states correlated with the 4*s* asymptote because of a faster time decay with respect to the first group (1.6 $\mu$s instead of 2.5 $\mu$s). They also suggested that the upper state of the transition might be $^1\Pi_g$ rather than $^3\Sigma_g^+$ because of the extension of the spectrum on the blue side. However as they admitted, this would not explain the qualitative difference observed in the rare gas series (the second absorption for $Ne_2^*$ and $Kr_2^*$ is continuous, whereas it is clearly structured in the case of $Ar_2^*$), since $^1\Pi_g$ states have the same bound character in the whole series. Moreover, the radiative lifetime of the $(1)0_u^+$ state was measured by Keto[43] (4.2 ns) and found to be of the nanosecond scale, whereas the lifetime of $(1)1_u$, $0_u^-$ was measured by different authors[43–48] in the range 2.88–3.22 $\mu$s. Thus, the weak variation in the time decay of the absorption signals for the two groups does not seem to be correlated with the different lifetimes of the possible initial states. In a subsequent paper, Kasama *et al.*[36] reconsidered those assumptions and concluded that both the first and second absorption groups had the same time-scale magnitude and should arise from the same initial state $(1)1_u$, $0_u^-(^3\Sigma_u^+)$. The upper states would correspond to the $\Omega$ components of the $(1)^3\Sigma_g^+$ state, namely $(1)1_g$ and $(1)0_g^-$. In our calculation, the spin–orbit splitting of this state is zero. It was found vanishing (of the order of 1 $cm^{-1}$) in the calculation of Teichteil *et al.*[11] The presently minimum to minimum calculated transition $(1)1_u$, $0_u^- \rightarrow (1)1_g$, $0_g^-$ is $T_e=7927$ $cm^{-1}$ with method *A*. It should emphasized that for the first time, those states deriving from $^3\Sigma_g^+$ are calculated to exhibit real minima with spin–orbit coupling rather than simple shoulders. Those minima are situated above the $4s(^3P_2)$ dissociation limit, but accept in our calculation two quasibound vibrational levels below the barrier top with transition maxima at respectively 7879 and 8053 $cm^{-1}$, separated by 174 $cm^{-1}$. This is in almost perfect agreement with the position and separation of the two most intense experimental peaks at 7899 and 8078 $cm^{-1}$ respectively. One should also notice that the 8078 $cm^{-1}$ peak is somewhat broader experimentally than the first one, which is consistent with the calculated position of this quasibound state, closer to the barrier top and with an expected shorter collisional lifetime due to tunneling through the barrier. We also remark that, based on energetic considerations only, the $(1)0_u^+ \rightarrow (1)0_g^+$ transition would not differ significantly from the latter assignment. The upper state is also (weakly) quasibound and the minimum to minimum transition is 8105 $cm^{-1}$ (method *A*). The oscillator strengths should be very similar for those singlet–singlet and triplet–triplet transitions with same core and orbital content. The main argument for discriminating the two hypotheses thus remains the large difference in the magnitudes of the radiative lifetimes of $(1)1_u$, $0_u^-$, and $(1)0_u^+$ initial states towards the $(1)0_g^+$ ground state which almost excludes transient absorption from the singlet state.

The most recent and extensive experimental studies[27,37–41] concern excitation of higher Rydberg states by single photon absorption from the lowest excimer state $(1)1_u$, $0_u^-(^3\Sigma_u^+)$. Various Rydberg series of gerade states with $[^2\Sigma_u^+]$ core, namely states deriving from $^3\Sigma_u^+$ $nl\sigma$ and $^3\Pi_g$ $nl\pi$, clearly assigned for $l=1$ (but also members of other series with $l\neq 1$) were observed. As indicated previously, states with the same $[^2\Sigma_u^+]$ core do not show significant fine structure splitting in the present calculation due to the neglect of spin–orbit coupling for the particle. Thus, theoretical transitions are very close either calculated in the $\Lambda$–$\Sigma$ coupling scheme or in the $\Omega$ scheme, including spin–orbit coupling. They are more sensible to the method used to calculate the exchange integral affecting mostly the depth of the $(1)^3\Sigma_u^+$ initial state of the transition. The basic experimental results of Sauerbrey *et al.*[37] and Kane *et al.*[27] are quite consistent. It can be seen in Table I that the calculated transitions are in good agreement with the experimental data. This correspondence provides a theoretical assignment of the observed transitions. Values obtained with method (*A*), overestimate the transitions by $\sim$300 $cm^{-1}$ whereas values obtained with method *B*, are generally very close to the experimental values, except for the higher states. In order to explain the overestimation of the transitions by a few hundredth $cm^{-1}$ for those higher states, one may invoke basis set uncompleteness (in particular the lack of the *f*-type functions) or the absence of two-electron integrals associated with $3p^5nd$ configurations. The most likely reason for the slightly lesser quality of the results obtained with method *A*, in line with the previous discussion about the singlet–triplet separations and the comparison with experiment for the lowest Rydberg state $(1)1_u$, $0_u^-$, is that method (*A*) tends to overestimate the exchange integral of the lowest configuration at short distance and thus overestimate by $\sim$300 $cm^{-1}$ (0.037 eV) the well depth of the $(1)^3\Sigma_u^+$ state and correlatively of the $(1)1_u$, $0_u^-$ state, initial state of the transitions.

## V. CONCLUSION

The pseudopotential hole-particle formalism introduced in paper I in its general formulation applicable to polyatomic rare gas excited systems has been in the present work experimented on the $Ar_2^*$ excimer, which appeared as a good benchmark since numerous theoretical and experimental data were available, at least for the lowest states and also for intra-Rydberg transitions. The method turns out to be very satisfactory for this case study.

From a qualitative point of view, with reference to *ab initio* calculations, the method provides a correct treatment of the Rydberg series associated with different ionic core parents and excited electrons in various Rydberg orbitals. Moreover, it is successful in dealing with various types of avoiding crossings, both those involving concerted and progressive core/orbital transformations which occur in orbital promotion processes and those which occur essentially at the configuration interaction level, characterized by weak avoid-

ance between two states spanned by molecular configurations differing simultaneously through the hole and the particle. The present work achieves a good reproduction of the behaviour of the electronic structure of the $Ar_2^*$ excimer in the energy range previously investigated in theoretical *ab initio* studies.

From a quantitative point a view, the present investigation is also very successful. For the lowest excimer states of ungerade symmetry dissociating into $Ar^*(4s)+Ar$, namely (1) $1_u,0_u^-$,(1)$0_u^+$, and (2)$0_u^+$, the present results are in very good agreement with the experimental data, even sometimes better than the *ab initio* studies which tend to underestimate the well depths of the two first excimer states (1) $1_u,0_u^-(^3\Sigma_u^+)$ and (1)$0_u^+(^1\Sigma_u^+)$. This is certainly due to the use of core interactions in the calculation taken from theoretical data in good concordance with experimental data for $Ar_2^+$, avoiding the difficult problem of treating the explicit correlation of the core electrons. Moreover, the calculation provides for the first time a description of the $(1)1_g,0_g^-(^3\Sigma_g^+)$ states after spin–orbit coupling as quasibound electronic states states containing respectively two quasibound vibrational levels. Those vibrational levels appear as excellent upper state candidates (in position and spacing) to explain the two main peaks of the infrared transitions group from $(1)1_u,0_u^-$ at 8065 $cm^{-1}$ investigated by Arai *et al.*[34] and Kasama *et al.*[35] The second group observed by the same authors is found to correspond to transitions from (1) $1_u,0_u^-$ to $\Omega$ fine structure components of the $(1)^3\Pi_g$ state, as in previous theoretical studies.

Beyond those states correlated with the first atomic excited configuration, the present method, allowing to use an extensive basis set for the unique active electron, has made possible to investigate excited states with increasing degree of excitation, namely several members of various Rydberg series, among which the most interesting are the gerade bound states with $[^2\Sigma_u^+]$ core. The transition energies of intra-Rydberg transitions starting from the lowest excimer state $(1)1_u0_u^-$ to those bound gerade states are found to be in close agreement with the concording experimental data of Kane *et al.*,[27] Conrad *et al.*[38] or Sauerbrey *et al.*[37] Due to the neglect of particle spin–orbit coupling, however, the present work does not allow to decide about different hypotheses and interpretations of some high resolution details in spectra where spin–orbit coupling and vibrational excitation are likely to interplay. An analysis in terms of natural orbitals and overlaps (holes and particles) has allowed to correlate most of the calculated Rydberg states at equilibrium ($R_e=4.6\ a_0$) with the orbitals of the united atom limit, namely the excited atomic orbitals of krypton. The trends observed in the evolution of the calculated Rydberg states with increasing excitation and going toward the ionization limit $Ar_2^+ + e$ indicate a small decrease of the equilibrium distance $R_e$ and an increase of the harmonic constant $\omega_e$, converging as expected to the ion values.

The present formalism thus appears as a promising tool in the treatment of Rydberg states. The accuracy of the calculation could be improved in several ways. Although the results already show a very satisfactory accuracy when compared with other types of calculations or experimental results, progress could certainly be achieved with a more accurate *a priori* knowledge of the ion potential curves, which still requires further *ab initio* studies. A second improvement may concern the evaluation of two-electron integrals. Both approximations used here and based on intra-atomic contributions, although not completely concording (essentially for the lowest excimer singlet–triplet splitting) provide realistic results in the range of theoretical and experimental data presently available. Possibly, one could improve the accuracy on dimers by computing those integrals *ab initio*. $3p^5nd$ two-electron contributions should be incorporated. Finally, one could think of introducing spin–orbit coupling for the active electron through pseudopotential techniques. This might be interesting for the heavier excimers such as $Xe_2^*$.

Beyond homonuclear dimers, applications are now in progress for $Ar_N^*$ clusters, starting with the determination of the electronic structure of $Ar_3^*$.


[1] J. S. Cohen and R. Schneider, J. Chem. Phys. **61**, 3230 (1974).
[2] W. R. Wadt, J. Chem. Phys. **68**, 402 (1978).
[3] R. P. Saxon and B. Liu, J. Chem. Phys. **64**, 3291 (1976).
[4] W. R. Wadt, P. J. Hay, and L. R. Kahn, J. Chem. Phys. **68**, 1752 (1972).
[5] W. C. Ermler, Y. S. Lee, K. S. Pitzer, and N. W. Winter, J. Chem. Phys. **69**, 976 (1978).
[6] M. C. Castex, M. Morlais, F. Spiegelmann, and J. P. Malrieu, J. Chem. Phys. **75**, 5006 (1981).
[7] F. X. Gadea, F. Spiegelmann, M. C. Castex, and M. Morlais, J. Chem. Phys. **78**, 7270 (1983).
[8] F. Spiegelmann and F. X. Gadea, J. Phys. **45**, 1003 (1984).
[9] P. A. Christiansen, K. S. Pitzer, Y. S. Lee, J. H. Yates, and W. C. Ermler, J. Chem. Phys. **75**, 5410 (1981).
[10] J. H. Yates, W. C. Ermler, N. W. Winter, P. A. Christiansen, Y. S. Lee, and K. S. Pitzer, J. Chem. Phys. **79**, 6145 (1983).
[11] C. Teichteil and F. Spiegelmann, Chem. Phys. **81**, 283, (1983).
[12] F. Grein and S. D. Peyerimhoff, J. Chem. Phys. **87**, 4684 (1987).
[13] H. U. Bohmer and S. D. Peyerimhoff, Z. Physik D **4**, 195 (1986).
[14] E. Audouard and F. Spiegelmann, J. Chem. Phys. **94**, 6102 (1991).
[15] Y. Mizukami and H. Nakatsuji, J. Chem. Phys. **92**, 6084 (1990).
[16] H. H. Michels, R. H. Hobbs, and L. A. Wright, J. Chem. Phys. **69**, 5151 (1978).
[17] P. Duplàa and F. Spiegelmann, J. Chem. Phys. **105**, 1492 (1996).
[18] R. S. Mulliken, J. Chem. Phys. **52**, 5170 (1970).
[19] M. Diegelmann, W. G. Wrobel, and K. Hohla, Appl. Phys. Lett. **33**, 525 (1978).
[20] M. J. Carvalho, Ph.D. thesis, Strasbourg, France, 1980.
[21] G. Zimmerer, J. Lumin. **18/19**, 875 (1979).
[22] F. Spiegelmann, Ph.D. thesis, Toulouse, France, 1983.
[23] Y. Tanaka and K. Yoshino, J. Chem. Phys. **53**, 2012 (1970).
[24] P. R. Herman, A. A. Madej, and B. P. Stoicheff, Chem. Phys. Lett. **134**, 209 (1987).
[25] P. R. Herman, P. E. LaRocque, and B. P. Stoicheff, J. Chem. Phys. **89**, 4535 (1988).
[26] K. T. Gillen, R. P. Saxon, D. C. Lorents, G. E. Ice, and R. E. Olson, J. Chem. Phys. **64**, 1925 (1976).
[27] D. J. Kane, S. B. Kim, D. C. Shannon, C. M. Herring, J. G. Eden, and M. L. Ginter, J. Chem. Phys. **96**, 6407 (1992).
[28] D. E. Freeman, K. Yoshino, and Y. Tanaka, J. Chem. Phys. **71**, 1780 (1979).
[29] Y. Matsuura and K. Fukuda, J. Phys. Soc. Jpn. **46**, 1397 (1979).
[30] Y. Matsuura and K. Fukuda, J. Phys. Soc. Jpn. **50**, 933 (1981).
[31] T. Möller, J. Stapelfeldt, M. Beland, and G. Zimmerer, Chem. Phys. Lett. **117**, 301 (1985).
[32] R. C. Michaelson and A. L. Smith, J. Chem. Phys. **61**, 2566 (1974).
[33] T. Tanaka *et al.*, Chem. Phys. Lett. **171**, 433 (1990).
[34] T. Oka, K. V. S. Rama Rao, J. L. Redpath, and R. F. Firestone, J. Chem. Phys. **61**, 4740 (1974).

[35] S. Arai, T. Oka, M. Kogoma, and M. Imamura, J. Chem. Phys. **68**, 4595 (1978).
[36] K. Kasama, T. Oka, S. Arai, H. Kurasu, and Y. Hama, J. Phys. Chem. **86**, 2035 (1982).
[37] R. Sauerbrey, H. Eizenhöfer, U. Schaller, and H. Langhoff, J. Phys. B **19**, 2279 (1986).
[38] N. Conrad, J. Muckenschnabel, and H. Langhoff, J. Phys. B **19**, 2279 (1986).
[39] K. P. Killeen and J. G. Eden, J. Chem. Phys. **84**, 6048 (1986).
[40] D. C. Shannon and J. G. Eden, J. Chem. Phys. **89**, 6644 (1988).
[41] N. Conrad, W. Giessl, C. Leisner, R. Tietz, and H. Langhoff, Z. Phys. D **16**, 71 (1990).
[42] E. Zamir, D. L. Huestis, H. H. Nakano, R. M. Hill, and D. C. Lorents, IEEE J. Quantum Electron. **QE15**, 281 (1979).
[43] J. W. Keto, R. E. Gleason, Jr., and G. K. Walters, Phys. Rev. Lett. **33**, 1365 (1974).
[44] N. Thonnard and G. S. Hurst, Phys. Rev. A **5**, 1110 (1972).
[45] P. Millet, A. Birot, H. Brunel, H. Dijols, J. Galy, and Y. Salamero, J. Phys. B **15**, 2935 (1982).
[46] T. Suemoto, Y. Kondo, H. Kanzaki, Phys. Lett. A **61**, 131 (1977).
[47] J. W. Keto, R. E. Gleason, Jr., G. K. Walters, T. D. Bonifield, and F. K. Soley, Chem. Phys. Lett. **42**, 125 (1976).
[48] P. Moutard, Ph.D. thesis, Lyon, France, 1986.